universität wien

MASTERARBEIT

Titel der Masterarbeit

Hsp70 and Hsp40 as immunohistochemical surrogate markers for DNA virus-infected cells

Verfasser

Jürgen Baldinger, BSc

angestrebter akademischer Grad

Master of Science (MSc)

Wien, 2012

Studienkennzahl lt. Studienblatt:	A 066 834
Studienrichtung lt. Studienblatt:	Masterstudium Molekulare Biologie
Betreuerin / Betreuer:	Ao. Univ.Prof. Dr. Jan Bauer

Curriculum vitae

Juergen Baldinger, BSc

born december 13th, 1975 in Gmunden, Upper Austria

MSc studies of Molecular Biology (*Neurosciences*)	University of Vienna, Medical University, Vienna	since 2010
MSc studies of Biology (*Nature Conservation and Biodiversity Management*)	University of Vienna	since 2011
BSc studies of Biology (*Anthropology*)	University of Vienna	2007 through 2011
journalistic work	various periodicals	2001 through present
Diploma studies of *Commercial Science*	Johannes Kepler University, Linz	1997 through 1998
University-entrance diploma	Handelsakademie, Gmunden	1996

Contact

Scheugasse 1/41
1100 Vienna (Wien)
0676 320 86 82
j.baldinger@gmx.at

Table of contents

List of frequent abbreviations 6
CV
Abstract 7
Introduction 8
Material and Methods 10
Human material 10
Sections 11
Blocking 12
Immunohistochemical labeling in general 12
Staining protocols in detail 13
Signal enhancement 15
Microscopy 15
Quantification of colocalization of Hsp70 and Hsp40 and viral markers 15
CSA solution 18
Qualitative PCR 18
Measurement of DNA concentration 19
Agarose gel electrophoresis 19
DNA extraction and quantification from paraffin sections 19
Laser-capture microdissection 20
DNA extraction from iLCM cells 20
Quantitative TaqMan real-time PCR 20
Qualitative TaqMan real-time PCR 21
Statistics 22
Results 23
Immunohistochemistry 24
General pathology of virus encephalitis 24
Qualitative description of Hsp70 and Hsp40 expression in viral encephalitis cases 25
Quantitative evaluation of Hsp70 and Hsp40 localisation in infected cells 27
Hsp70 reactivity 27
Hsp40 reactivity 28
CMV
Hsp70 reactivity 29
Hsp40 reactivity 30
PML
Hsp70 reactivity 32
Hsp40 reactivity 34
HSV-1
Hsp70 reactivity 37
EBV
Hsp70 reactivity 39
Genetics:
Detection of viral DNA in immunohistochemically untreated sections 42
Detection of viral DNA in immunohistochemically treated sections 44

Detection of viral DNA in laser-capture microdissected stained cells 47
Pre-experiment 48
Microdissection in CMV 49
Microdissection in PML 51
Interpretation 53
Immunohistochemical testing of Hsp70 and Hsp40 by virus-specific markers 55
Virus-specific PCR detection of isolated Hsp70 and Hsp40 positive cells 55
Conclusion and future prospects 56
Acknowledgments 57
Literature 57

Table of figures

Fig. 1: Polyclonal antibodies 13
Fig. 2: Monoclonal antibodies 13
Fig. 3: Light-microscopy of Hsp40 staining in CMV and of Hsp70 staining in PML 24
Fig. 4: Graphical representation of nuclear Hsp70 reactivity evaluation in examined encephalitides 28
Fig. 5: Graphical representation of nuclear Hsp40 reactivity evaluation in examined encephalitides 29
Fig. 6: Graphical representation of Hsp70 reactivity evaluation in CMV 30
Fig. 7: Graphical representation of Hsp40 reactivity evaluation in CMV 31
Fig. 8: Confocal laser microscopy of Hsp70 and Hsp40 colocalizations in CMV 32
Fig. 9: Graphical representation of Hsp70 reactivity evaluation in PML cases (by α-SV40 antibody) 34
Fig. 10: Graphical representation of Hsp40 reactivity evaluation in PML cases (by α-SV40 antibody) 35
Fig. 11: Graphical representation of Hsp70 reactivity evaluation in PML cases (by α-PAb2003 antibody) 35
Fig. 12: Confocal laser microscopy of Hsp70 and Hsp40 colocalizations in PML 37
Fig. 13: Graphical representation of Hsp70 reactivity evaluation in HSV-1 38
Fig. 14: Confocal laser microscopy of Hsp70 colocalizations in HSV-1 and light-microscopic assessment of colocalizations of HSV-1 infected and $Hsp70^{+}$ cells on separate sections 39
Fig. 15: Graphical representation of Hsp70 reactivity evaluation in EBV 40
Fig. 16: Graphical representation of Hsp70 reactivity evaluation in EBV 41
Fig. 17: Confocal laser microscopy of Hsp70 colocalizations in EBV 41
Fig. 18: Analytic DNA gel electrophoresis for DNA quality analysis of unstained samples 44
Fig. 19: Analytic DNA gel electrophoresis for comparison of DNA quality analysis of RE sections 47
Fig. 20: Screen-shot from laser-capture application 48

Table directory

Tab. 1: Case overview of examined infections 10
Tab. 2: Antibodies used for immunohistochemical Hsp70 and Hsp40 labeling 16
Tab. 3: Recipes used in immunohistochemistry 17
Tab. 4: Human β-actin primer sequences 19
Tab. 5: TaqMan real-time PCR reaction mix 18
Tab. 6: Primers and probes used for TaqMan real-time PCR 21
Tab. 7: Real-time PCR set up 22
Tab. 8: Overview on relative frequencies of virus-marked cells with nuclear Hsp70 reactivity per case in evaluated encephalitides 28
Tab. 9: Overview on relative frequencies of virus-marked cells with nuclear Hsp40 reactivity per case in evaluated encephalitides 29
Tab. 10: Location and relative frequencies of Hsp70 reactivity in virus-marked cells in CMV cases 30
Tab. 11: Location and relative frequencies of Hsp40 reactivity in virus-marked cells in CMV cases 31
Tab. 12: Location and relative frequencies of Hsp70 reactivity in virus-marked cells in PML cases (by α-SV40 antibody) 33
Tab. 13: Location and relative frequencies of Hsp40 reactivity in virus-marked cells in PML cases (by α-SV40 antibody) 34
Tab. 14: Location and relative frequencies of Hsp70 reactivity in virus-marked cells in PML cases (by α-PAb2003 antibody) 35
Tab. 15: Location and relative frequencies of Hsp70 reactivity in virus-marked cells in HSV-1 cases 38
Tab. 16: Location and relative frequencies of Hsp70 reactivity in virus-marked cells in EBV cases (by α-LMP antibody) 40
Tab. 17: Location and relative frequencies of Hsp70 reactivity in virus-marked cells in EBV cases (by α-EBV zebra antibody) 40
Tab. 18: Photospectrometric determination of DNA concentrations of IHC untreated samples 43
Tab. 19: Photospectrometric determination of DNA concentrations of Hsp70 stained samples 45
Tab. 20: Real-time PCR analysis of IHC untreated contrasted to treated sections 46
Tab. 21: Photospectrometric determination of DNA concentrations of RE comparison 47
Tab. 22: Photospectrometric determination of DNA concentrations of laser-captured Hsp70^{+} cells 49
Tab. 23: Qualitative real-time PCR by TaqMan probes in PML case 49
Tab. 24: Qualitative real-time PCR by TaqMan probes of Hsp40^{+} cells in CMV cases 50
Tab. 25: Repeated dissection of CMV 559-92-11 50
Tab. 26: Qualitative real-time PCR by TaqMan probes of Hsp40^{+} cells in PML cases 52/53
Tab. 27: C_q mean differences in the different fractions 53
Tab. 28: C_q means with eliminated samples 54

List of frequent abbreviations

CMV	Cytomegalo virus
EBV	Epstein-Barr virus
EEG	electroencephalography
JC virus	John Cunningham virus
HIV	Human Immunodeficiency virus
HSV	Herpes Simplex virus
IHC	Immunohistochemistry
iLCM	Immuno-laser-capture microdissection
MHC	Majorhistocompatibilty complex
MV	Measles virus
PML	Progressive Multifocal Leukencephalopathy
RE	Rasmussen encephalitis
SSPE	Subacute sclerosing panencephalitis
SV40	Simian *v*acuolating virus 40
TBE	Tick-borne virus encephalitis

Abstract

Some encephalitides are suspected to be initiated by viruses although after analysis no actual evidence for a virus is found. As general virus markers are not available heat-shock proteins Hsp70 and Hsp40 could act as surrogate markers for DNA virus-infected cells in vivo. Immunohistochemical analysis of encephalitic human brain tissue showed clear upregulation and nuclear translocation of these chaperones In CMV and JC virus infected cells. Such coincidence was not found in HSV-1 infected cells and in EBV preparations although this has been already described in vitro. Real-time PCR by virus-specific primers detected presence of viral DNA in laser-capture microdissected $Hsp40^{+}$ cells in prinicipal thereby confirming these findings although uncertainties regarding this procedure remained.

Zusammenfassung (abstract german)

Einige Enzephalitiden stehen im Verdacht, durch Viren verursacht zu werden, auch wenn nach Untersuchungen kein Beleg dafür gefunden wurde. Da keine allgemeinen Virus-Marker bekannt sind, könnten die heat-shock-Proteine Hsp70 und Hsp40 als Surrogat-Marker für DNA-Virus-infizierte Zellen dienen. In der immunhistochemischen Analyse enzephalitischen, humanen Hirngewebes zeigen diese Chaperones in CMV- und JC Virus-infizierter Zellen sowohl klare Aufregulation als auch Translokation in den Zellkern. Dieser Zusammenhang konnte in HSV 1- sowie in EBV-infizierten Zellen nicht beobachtet werden, obwohl bereits beschrieben in vitro. Bestätigt wurden diese Ergebnisse dadurch, dass durch real-time PCR mit Virus-spezifischen *primers* das Vorliegen viraler DNA in per *laser* mikrosezierten $Hsp40^{+}$ Zellen prinzipiell detektiert wurde; Restunsicherheiten konnten nicht ausgeräumt werden.

Introduction

The cause of certain encephalitides as for example Rasmussen encephalitis (RE) still remains unknown. RE, named after american neurologist Theodore Brown Rasmussen (1910 – 2002), is a neurodegenerative, unilateral disease characterized by chronic epilepsy with enduring inflammation, intractable seizures and progressive impairment of neurologic functions. In RE, an initial prodromal phase is followed by an acute phase eventually ending in a residual stage. No exact epidemiological data, e. g. regarding incidence. RE is listed as "rare disease" by the US Office of Rare Diseases of the National Institute of Health. Only medical conditions that affect less than 200,000 people in the US population fall in this category. On average, disease manifests at an age of 6 years[1]. No gender predominance is observed. Early tentative diagnosis is possible 4 to 6 months from first symptoms by association of partial seizures with focal electroencephalography (EEG) and neuroimaging changes. When diagnostic criteria as suggested by Granata et al are fulfilled brain biopsy can be unnecessary[2]. The neurologic deterioration that strongest occurs in the acute phase is related to one hemisphere. Lastly is it reaching hemiplegia, hemianopia and, in case the dominant hemisphere is concerned, aphasia. Hemispherectomy is considered the most effective therapy[3] albeit at the same time reckoned the most invasive surgical intervention today.

Cell and histopathological alterations in RE seem to make a viral cause supposable. These changes regard to microglial nodules varying in number from area to area[4] and astrocytic apoptosis[5] both in cortical and in white matter areas. Granzyme B^+ lymphocytes partly were found close to astrocytes bordering astrocyte-deficient lesions. A specific attack of astrocytes is also suggested as they show upregulation of majorhistocompatibility complex (MHC) class I expression. For Bauer et al these findings are consistent with common viral encephalitides caused by e. g. Cytomegalo virus (CMV), JC virus (provokes Progressive Multifocal Leukencephalopathy, PML) or Human Immunodeficiency virus (HIV). As no general virus markers are available at the moment the search for a virus as potential cause for RE proves to be difficult. Heat-shock proteins could deliver a solution to this problem.

Heat-shock protein translocation in virus-infected cells

ADP-bound Heat-shock protein70 (Hsp70) catalyzes the folding of nascent peptides and unfolded substrates, thus, making it an important cytosolic chaperon in times of cellular stress as in virus infection. Hsp40 functions as its interacting hydrolysis partner by delivering unfolded substrates to ATP-bound Hsp70 and binding to the latter. This increases hydrolysis of ATP-Hsp70. This action is later reversed by a nucleotide exchange factor. Repeated binding and ATP hydrolysis cycles help to prevent premature folding and aggregation of nascent peptides and therefore providing timely protein maturation throughout the cell.

In-vitro studies with Herpes Simplex Virus 1 (HSV-1) showed intranuclear foci enriched in chaperones, e. g. Hsc70. These foci that often form adjacent to viral replication compartments were designated by Burch and Weller "virus-induced chaperone-enriched (VICE) foci[6] ". Besides chaperones, 20S proteasome and ubiquitin are reorganized in these VICE foci. Livingston et al.[7] suppose these compartments are sites of protein remodeling and quality control. These compartments would be similar to nuclear inclusion bodies (IB) that can be observed in presence of too many misfolded proteins. The terminology for nuclear or cytoplasmatic compartments of protein aggregations remains diverse. While in Rabies virus infection IB are refered to as "Negri bodies" the term "owl eyes" is used in CMV and "Warthin finkeldey bodies" in Measles virus. Heat-shock proteins as Hsp70, Hsp40, and others could display a therapeutic target. It was demonstrated that inhibition of Hsp90 present in VICE foci and replication compartments blocks viral DNA synthesis, mislocalizes DNA polymerase and degrades viral polymerase.[8]

Translocation of stress proteins as Hsp70 and Hsp40 to the nucleus is observed during overproduction of nuclear proteins. Koskinen et al reported that transcriptional regulators such as *myc* proteins play a role in nuclear translocation, independent from cell cycle or heat shock stress[9]. Upregulated protein production and assembly is also required when the cell is infected by viruses. In Papilloma virus-infected cells, Florin et al showed the need of minor capsid protein L2 for Hsp70 to get relocated to the nucleus. An active complex is formed accumulating in nuclear bodies, also called promyelocytic leukemia bodies or PODs (promyelocytic leukemia oncogenic domains) or nuclear domain (ND) 10[10]. Brown et al see evidence for a transport of Hsp70 and other cellular factors to lipid-raft membranes within IB where the virus polymerase comples is found[11]. For biochemical and genetic details of Hsp70 chaperons please see the review of Mayer et al[12], and also for the comprehensive role of Hsp70 chaperones in viral lifecycle this author gives a broad overview[13]. Therapeutically rewarding could be the observation that some bacteriophages like phage λ only need host-encoded chaperones whereas other viruses such as Simian virus 40 (SV40) also encodes own factors. The latter proteins could contain virally specific elements not found in host-encoded counterparts[14].

Although translocation of heat-shock proteins to the nucleus has been shown in *in vitro* studies, no data exist that this translocation also is visible *in situ*. Identification of nuclear localization of Hsp40 and/or Hsp70 could be used as a possible marker to detect virus-infected cells in encephalitic cases with unknown but suspected viral aetiology. Furthermore, in suspected viral diseases such as RE such a marker could be used to isolate alleged infected cells by laser capture. Genomic analysis by techniques as PCR or microarray analysis would be possible. Aim of this work was to demonstrate that Hsp40 and Hsp70 translocation can be observed *in situ* in brains of known viral aetiology and to show that DNA and/or RNA isolated from $Hsp40^+$ or $Hsp70^+$ cells indeed can be used for analysis and identification of a certain virus.

Material and Methods

Human material

For this study paraffin embedded brain material from the archives of the Department of Neuroimmunology, Center for Brain Research was used. Autopsy brain tissue containing CMV, PML, Epstein-Barr virus (EBV), and HSV-1 was examined. Also analyzed was tissue with RNA viruses Measles virus (MV, from an SSPE patient) and Tick-borne virus (TBV) as well as retrovirus HIV (Tab. 1).

***Tab. 1**: Case overview of examined infections*

	PML	CMV	HSV	EBV	TBV	MV	HIV
sample size	n = 7	n = 6	n = 6	n = 2	n = 2	n = 2	n = 3
case numbers	12-93-2 97-93-8 47-93-8 103-93-8 278-93-6 358-93-6 359-93-7A2	62-94-9 234-93-1 290-93-5 430-93-7 455-92-7B 559-92-11	67-83-2 204-83-4 237-91-5 330-82-4 514-82-10 529-84-6	130-07-1 281-00-1	245-90-1 6942-96	63-94-11 260-82-9	53-94-1 122-3-98-1 428-93-1

The following encephalitogenic virus infections were evaluated:

CMV

Human CMV, alternatively known as Human herpesvirus 5 (HHV-5) belongs to Herpesviridae (Herpes viruses) and exhibits a double-stranded (ds) DNA genome. Usually unnoticed in healthy persons CMV can cause life-threatening infections for the immunocompromised as HIV-infected people. The virus can resist latent within the body for long periods of time. Only HIV-associated CMV infections were inspected.

PML

Opportunistic agent of PML is the dsDNA virus JC virus from the genus polyomavirus in the family of polyomaviridae. As Simian vacuolating virus 40 (SV40) large T antigen and JC virus large T antigen cross-react serologically, detection of the latter is possible by using an SV40 polyclonal antibody. While all other factors necessary for SV40 replication are encoded by

the infected host cell, the SV40 protein is the only viral protein brought in. As in CMV, only HIV-associated PML was examined.

HSV-1

As in CMV and PML, HIV-associated HSV-1 infections were subjected to investigation. HIV-1 infections are often accompanied by opportunistic HSV-1 and HSV-2 infections. The prevalences frequently exceed those in the general population. Recent studies on co-occurrence of HSV-2 and HIV-1 show a seroprevalence of 50 – 90 % in some populations as Strick et al reported.[15] A possible explanation responds to the shared route of sexual transmission of the two viruses. HSV-1 can cause focal encephalitis. In the general population a relatively low incidence of 2 to 4/1.000.000 individuals/year is observed. Age distribution occurs bimodally there: More than 80 % of cases are observed in patients less than 20 or greater than 50 years of age; sexes are affected equally[16 17].

EBV

EBV belongs to the family of herpesviruses and is regarded one of the most common human and worldwide occurring viruses. The US National Center for Infectious Diseases estimates that 95 % of adults between 35 and 40 are infected. Infants become susceptible as their exposition to maternal antibodies ends after birth. Infected children mostly develop no or just mild symptoms but the majority of infections appears during adolescence or young adulthood. In 35 to 50 % of cases infectious mononucleosis (symptoms: fever, sore throat, swollen lymph glands, sometimes swollen spleen or liver, seldom problems of the heart or central nervous system) is caused that is rarely fatal. EBV stays dormant or latent in some cells in the throat and blood of the patient during lifetime. A few cells persist in the immune system leading to rare cancers Burkitt's lymphoma and nasopharyngeal carcinoma in some carriers[18].

Immunohistchemistry

<u>Sections</u>

All immunohistochemical stainings were performed on paraffin sections of 3 to 5 µm thickness. Sectioning was carried out by a sledge microtome (Leica Microsystems). Cut sections were stretched in water and collected on coated glass slides (Superfrost Plus,Thermo Schientic). Subsequently, slides were baked in an oven (4 to 6 hrs. at 56° C). Before application sections were deparaffinized in Xylene (Sanova 3410.5000PE) twice for 15'. Xylene is an organic solvent consisting of an isomere mixture of *o*rtho- (1,2-dimethylbenzene), *m*eta- (1,3-dimethylbenzene), and *p*ara- (1,4-diemethylbenzene)xylene.

After rehydrating in a graded ethanol series endogenous peroxidase was blocked by 0.2 % of 30 % H_2O_2 (Merck 1.07210) in methanol (VWR 20847.307). Antigen retrieval by steaming in a household food steamer device (MultiGourmet FS 20, Braun) was carried out. Therefore, sections were put into plastic coplin jars filled with their respective buffers and steamed for 60' or 90', respectively. Buffers were either citrate buffer (pH = 6.0) or EDTA buffer (pH = 9.0). As a washing buffer Tris-buffered saline (TBS) was applied. Recipes are listed below in detail.

Blocking

After antigen retrieval by steaming the sections were blocked with 10 % fetal calf serum (FCS, dissolved in washing buffer (Dako, Denmark)) for 20'. FCS excels as being poor in antibodies but rich in various proteins like growth factors and is therefore suitable for many cell biological applications. Based on van der Waals-forces, FCS suppresses unspecific antibody binding due to hydrophobic interactions. These can occur between macromolecules with surface tension values lower than that of water. FCS contains proteins identical to those in the secondary antibody therefore preventing its unspecific binding. Ionic interactions that tend to aggravate hydrophic effects as well as adherence effects on glass and plastic surfaces also seem to contribute to background staining.

Immunohistochemical labeling in general

Staining was carried out by indirect labeling, a standard protocol in contemporary immunohistochemistry. An enzyme-labeled secondary antibody binds to a primary antibody recognizing a specific epitope on the antigen of interest. Primary antibodies in cases of fluorescent microscopy were diluted in Dako Antibody Diluent, while non-fluorescent antibodies and secondary fluorescent antibodies and fluorophors were diluted in 10 % FCS. Continuously, primary antibodies were applied twice: first over night (o/n) at 4 ° C, followed by an incubation of another hour at room temperature (RT) after washing with TBS. For immunohistochemical stainings polyclonal as well as monoclonal Hsp70 antibodies were adopted. While polyclonal antibodies (pAb, Fig. 1) originating from different B cell lines bind to the various epitopes of a specific antigen monoclonal antibodies (mAb, Fig. 2) are more specific. Produced from a cloned single B cell they have "monovalent affinity" causing interaction only with one specific antigenic determinant.

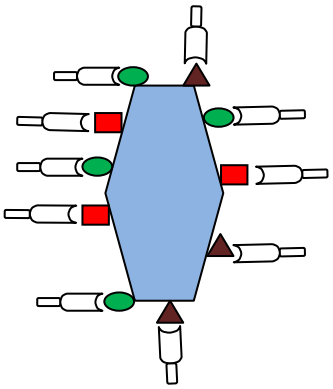

***Fig. 1**: Polyclonal antibodies derived from B cell populations from different animals recognize all epitopes available on their antigen*

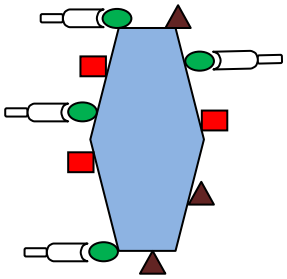

***Fig. 2**: Monoclonal antibodies derived from a single B lymphocytic cell line recognize only one specific epitope on their antigen*

Substrate for the Horseradish Peroxidase (HRP) was either DAB (3,3'-diaminobenzidine) delivering a colorimetric product in the presence of the DAB-oxidizing H_2O_2. Alternatively, AEC (3-Amino-9-Ethylcarbazol) was applied resulting in red staining. Here, too, H_2O_2 was adopted to enable the catalysis of AEC by HRP. Alkaline Phosphatase stainings were developed by Luxol Fast Blue BB.

Staining protocols in detail

CMV

Various pre-experiments suggested an antigen retrieval with EDTA (pH = 9.0) of 90' steaming. After blocking as described above polyclonal α-Hsp70 antibody (Ab) and CMV specific antibody were applied (Tab. 2). Monoclonal viral marker was followed by biotinylated anti-mouse Ab and fluorophor streptavidin-conjugated Cy2. Hsp70 was stained by incubating sections in anti-rabbit-Cy3. Nuclei were stained by To-Pro3-Iodide (pretreatment 1 M HCl for 30', then incubation 1 : 1,000 in PBS, 15'). This carbocyanine monomer nucleic acid stain with far-red fluorescence similar to Alexa Fluor 647 or Cy5 dyes recognizes dsDNA. Sections were covered in Pro-Long gold anti-fade reagent. For recipes of substrates used in immunohistochemistry see Tab. 3.

PML (by α-SV40 large T antigen antibody)

Staining procedure for PML slides comprehended 90' EDTA (pH = 9,0) pretreatment and blocking as described above. Next, section was incubated with polyclonal SV40 for detection of the JC virus (Tab. 2). Together with this virus marker monoclonal Hsp70 was added.

Primary antibodies were subsequently incubated with biotinylated α-rabbit secondary antibody and streptavidin-conjugated Cy2. α-Hsp70 antibody was displayed by incubation with α-mouse-Cy3. α-SV40 antibody was signal enhanced by CSA, please see respective section below. Nuclei counterstaining and covering was done as in CMV cases.

PML (by α-PAb2003 antibody)

Staining protocol for confirmation of JC virus infection by monoclonal α-PAb2003 antibody was in principal identical to the section before referring to PML detection by α-SV40 antibody, including signal enhancement by CSA amplification (Tab. 2). PAb 2003 antibody reacts to JCV early proteins[19]. Nuclei counterstaining and covering was done as in CMV cases.

HSV-1

Pretreatment and blocking was carried out as in the previous sections. Polyclonal α-HSV and monoclonal α-Hsp 70 antibody were brought up followed by secondary antibody incubation as in PML cases (Tab. 2). Nuclei counterstaining and covering was done as in CMV cases.

EBV (by α-EBV LMP)

Pretreatment and blocking was carried out as in the previous staining protocols above. Monoclonal primary viral antibody α-EBV LMP was used and combined with polyclonal α-Hsp70 antibody (Tab. 2). Secondary antibody was used as in PML cases. Nuclei counterstaining and covering was done as in CMV cases.

EBV (by α-EBV zebra)

Protocol as in section before except use of α-EBV zebra as viral marker (Tab. 2).

Measles virus

Staining procedure comprehended 60' EDTA (pH = 9,0) pretreatment and blocking as described above. The monoclonal FLAG-antibody 2B4 was taken for detection of virus-infected cells (Tab. 2). Secondary antibody was applied as in the CMV cases.

HIV

Pretreatment was steaming in EDTA (pH = 9.0) for 60' for antigen retrieval. Monoclonal mouse antibody p24 was used combined with polyclonal Hsp antibodies as described in the CMV cases above (Tab. 2).

Signal enhancement

For signal enhancement of α-SV40 and α-PAb2003 antibody in PML and α-p24 antibody in HIV avidin-labeled horseradish peroxidase (HRP) was used, succeeded by CSA ("catalyzed signal amplification", 1 : 1000, 20'). This tyramide amplification reagent leads to the aggregation of biotinylated tyramine after reaction with an oxidizing agent as HRP and H_2O_2 added before[20]. Phenolic compound tyramine is the aminated form of the aromatic amino acid tyrosine. Conversion to a highly reactive radical species occurs. In this state electron-rich molecules like proteins are bound in the surroundings of the antigen-antibody complex hence amplifying the signal. For details of the chemical reaction please see Schmitt et al[21].

Microscopy

For quantitative assessment by fluoresence microscopic detection the Leica TCS SP5 was used. All pictures of CMV, EBV, HS1V, and PML cases as listed below were taken in format of 2.048 x 2.048 pixels and scanned with 700 Hz. Sequential scanning (first Cy2 and To-Pro, then Cy3) was chosen to avoid wrong positive excitation from lasers emitting light at different wavelengths. Magnification was 400x. Line average to increase signal/noise ratio was 4x.

Quantification of colocalization of Hsp70 or Hsp40 and viral markers

Lesions with an aggragation of virus-positive cells were scanned, photographed and counted for Hsp70 and Hsp40 reactivity. These lesions originated from all over the section to achieve good representativity; between 100 and 200 cells per section were analyzed where available. Cells with virus marker reactivity were examined for colocalizations of Hsp70 and Hsp40 reactivity. Such coincidence of both Hsp70 or Hsp40 and virus marker reactivity was divided into the following seven categories:

I. cells with virus marker signal in the nucleus
   - Hsp70 and Hsp40 reactivity only in nucleus
   - Hsp70 and Hsp40 reactivity both in nucleus and cytoplasm
   - Hsp70 and Hsp40 reactivity only in cytoplasm
   - no Hsp70 and Hsp40 reactivity

II. cells with virus marker signal cytoplasmatically
- Hsp70 and Hsp40 reactivity in nucleus
- Hsp70 and Hsp40 reactivity in cytoplasm
- no Hsp70 and Hsp40 reactivity

***Tab. 2**: Antibodies used for immunohistochemical Hsp70 and Hsp40 labeling*

CMV
Pretreatment: steaming EDTA (pH = 9.0) for 90'

Antigen	Dilution	Ab type	Target	Source
CMV	1 : 2,500	mouse, mc	HCMV	Chemicon
Hsp70	1 : 1,500	rabbit, pc	Hsp70	Stressgen
Hsp40	1 : 100	rabbit, pc	Hsp40	Enzo

PML by SV40 large T antigen
Pretreatment: steaming in EDTA (pH = 9.0) for 90'

Antigen	Dilution	Ab type	Target	Source
SV40*)	1 : 40,000	rabbit, pc	SV40 large T antigen	Dr. Höftberger, AKH
Hsp70	1 : 400	mouse, mc	Hsp70	C92
Hsp40	1 : 750	rabbit, pc	Hsp40	Enzo

PML by Pab 2003
Pretreatment: steaming in EDTA (pH = 9.0) for 90'

Antigen	Dilution	Ab type	Target	Source
PAb 2003	1 : 2,000	mouse, mc	JCV large T antigen	Dr. Frisque
Hsp70	1 : 1,500	rabbit, pc	Hsp70	Stressgen

HSV I
Pretreatment: steaming EDTA (pH = 9.0) for 90'

Antigen	Dilution	Ab type	Target	Source
HSV	1 : 500	rabbit, pc	HSV1	Dr. Budka, AKH
Hsp70	1 : 400	mouse, mc	Hsp70	C92
Hsp40	1 : 750	rabbit, pc	Hsp40	Enzo

EBV by EBV Zebra
Pretreatment: steaming EDTA (pH = 9.0) for 90'

Antigen	Dilution	Ab type	Target	Source
EBV Zebra	1 : 40	mouse, mc	BZLF1-encoded replic. activ.	Dako
Hsp70	1 : 1,500	rabbit, pc	Hsp70	Stressgen
EBV	1 : 750	rabbit, pc	Hsp40	Enzo

EBV by EBV LMP
Pretreatment: steaming EDTA (pH = 9.0) for 90'

Antigen	Dilution	Ab type	Target	Source
EBV LMP	1 : 40	mouse, mc	latent membrane protein	Dako
Hsp70	1 : 1500	rabbit, pc	Hsp70	Stressgen

Measles virus (SSPE)
Pretreatment: steaming in EDTA (pH = 9.0) for 60'

Antigen	Dilution	Ab type	Target	Source
2B4 FLAG	1 : 250	mouse, mc	nucleocapsid protein 2B4	D. Gilden
Hsp70	1 : 1,500	rabbit, pc	Hsp70	C92
Hsp40	1 : 250	rabbit, pc	Hsp40	Enzo

HIV
Pretreatment: steaming in EDTA (pH = 9.0) for 60'

Antigen	Dilution	Ab type	Target	Source
p24*)	1 : 1,000	mouse, mc	capsid protein p24	Dako
Hsp70	1 : 1,500	rabbit, pc	Hsp70	Stressgen
Hsp40	1 : 750	rabbit, pc	Hsp40	Enzo

**) CSA amplified*
pc … polyclonal
mc … monoclonal

***Tab. 3**: Recipes used in immunohistochemistry*

PFA	4 % PFA were solved in 50 % "Sörensen buffer" (= PBS without NaCl, dilution in A. dest).
Tris buffer stock	0.5 M Tris(hydroxymethyl) Limahl (2-Amino-2-hydroxymethyl-propane-1,3-diol), abbreviated "Tris" and 3.1 M NaCl were solved in A. dest. For usage purposes the stock was diluted 1 : 20.
EDTA buffer stock	10 mM Tris and 1 mM EDTA were solved in A. dest. The pH was set to ph = 9.0 or 8.5, respectively by adjustment with HCl. Working solution for one cuvette was 2.5 ml of EDTA buffer stock with 47.5 ml A. dest.
Citrate buffer	1 M citrate was solved in A. dest. The pH was set to 6.0 by adjustment with NaOH.

TBS including NaCl	25 mM Tris buffer and 150 mM NaCl were solved in A. dest. The pH was set to 7.5 by adjustment with HCl.
PBS stock (= "Sörensen buffer")	0.04 M NaH_2PO_4 and 0.16 M Na_2HPO_4 were solved in A. dest. The pH was set to 7.4 by adjustment with HCl. For usage purposes the stock was diluted 1 : 4.
Horseradish Peroxidase – Developing substrates	**DAB stock** 25 mg 3,3'diaminobenzidine-tetra-hydrochloride (DAB) were solved in 1 M PBS buffer. For usage purposes the stock was diluted 2 : 100 in 50 ml PBS. This solution was stirred and filtrated. 16.5 µl of 30 % H_2O_2 were added. **AEC stock** 4 mg AEC/ml were solved in Dimethylformamide. **AEC solution** 0.05 M Sodium acetate buffer with pH set to 4.9 by adjustment with glacial acetic acid and 780 mg AEC stock were solved in 45 ml Dimethylformamide. Finally, 0.5 ‰ of 30 % H_2O_2 were added.
Alkaline Phosphatase – Developing substrates	**Fast Blue** 0.1 M Tris-HCl with a ph set to 8.5 by adjustment with HCl, 4 % $NaNO_2$, 1 M Levamisole, 6.5 mg/50 ml Naphtol-AS-MX-phosphate, 307.5 l/50 ml Dimethylformamide, 12.5 mg/50 ml Fast Blue and 2M HCl were solved in 50 ml Tris-HCl. Temperature of the solution was set to 37° C.

CSA solution

For CSA stock solution borat buffer was produced by solving 0.1545g boric acid in 50 ml A. dest. The pH was set to pH 8.0 by adjustment with NaOH. For usage purposes 15 mg sulpho-NHS-LC-Biotin were solved in 6 ml borat buffer. Then, 4.5 mg Tyramin were added and the solution was stirred O/N at RT. Eventually, the solution was filtered with a 0.45 µm filter.

Qualitative PCR

Qualitative PCR for assessment of DNA quality by using human β-actin specific primers was performed with the reaction mix listed below (Tab. 4, 5). 40 amplification cycles were carried out in the thermocycler.

***Tab. 4**: Human β-actin primer sequences*

5' – 3'
for: TTG ACT CAG GAT TTA AAA ACT GG
rev: AGG GAC TTC CTG TAA CAA CGC

***Tab. 5**: TaqMan real-time PCR reaction mix*

FastStart Taq DNA Polymerase	5 U/µl in storage and dilution buffer	0,4 µl
PCR Reaction Buffer	10x conc. with 20 mM $MgCl_2$	5 µl
Primers	100 pmol/ml stock conc.	1 µl
dNTPs	10 mM each	1 µl
sample material	varied	1 µl
H_2O		40,6 µl
		50 µl

Denaturation temperature for PCR detection of human β-actin was set to 95° C (first 10', then each step for 30''), annealing temperature was 55° C (each step for 30'') and elongation was performed at 72°C (each step for 30'').

Measurement of DNA concentration

All quantifications of DNA concentrations were carried out by using the NanoDrop2000 spectrometer, a micro-volume UV-Vis spectrophotometer for nucleic acid and protein quantification. DNA, RNA (A260), and Protein (A280) concentrations as well as sample purity (260/280 ratio) were measured.

Agarose gel electrophoresis

Analytic electrophoresis for verification of PCR products were carried out by running an agarose gel (2 % agarose in Tris-acetate-EDTA buffer). Ethidium bromide (8 mg/200 ml) was added directly to the gel. Voltage 100 V, current 200 mA, durage 75'.

DNA extraction and quantification from paraffin sections

All DNA extractions were performed using the Allprep DNA/RNA FFPE protocol from Qiagen.

Laser-capture microdissection

Nuclease and human nucleic acid free and 1.4 µm thick PET-membrane slides of 76 x 26 mm destined for use in laser capture microdissection were taken as object slides for paraffin sections. The laser-capture was done with the mmi CellCut Plus device at the Department of Applied Anatomy at the enter of Anatomy and Cell Biology in Vienna.The procedure including immunohistochemical marking of cells or tissue is referred to as "immuno-LCM (iLCM, LCM standing for laser-capture microdissection)".

DNA extraction from iLCM cells

DNA from micro-dissected cells was extracted complying with the Qiagen protocol "Isolation of Genomic DNA from Laser-Microdissected Tissues". Deviant from the protocol the proteinase K incubated samples were kept on 56 ° C O/N without agitation. 1 µl of carrier RNA (courtesy of the Department mentioned) was added to the AL-buffer (see step 5 of protocol)

Quantitative TaqMan real-time PCR

Real-time PCR for quantification of virus-load in paraffin-embedded tissue sections of PML, HS1 and Epstein-Barr virus patients was performed by Prof. Stephan Aberles group in the Department of Virology of the AKH, Vienna. TaqMan probes were used to elicit the fluorescence signal for calculation of a standard curve to quantify the probes. For this TaqMan based Real-time PCR 5 µl of DNA were added to the amplification mixture, using TaqMan universal PCR master mix (PE Applied Biosystems), yielding a total volume of 25 µl. For primers and probes please see Tab. 6. The amplification was performed on iQ cycler (Bio-Rad, Hercules,CA) or on ABI 7300 Real-Time PCR System (Applied Biosystems, Foster City, CA) with the following uniform cycling conditions: 3 min at 50°C, 10 min at 95°C followed by 45 cycles of 95°C for 15 sec, 55°C and 72°C each for 30 sec.

***Tab. 6**: Primers and probes used for TaqMan real-time PCR*

virus sequence 5´-3´ primer 1 primer 2 probe	**conc. per reaction in pmol**	**target region**	**references**
Herpes simplex virus type 1		UL-42	Aberle
CCG TAG TTT CTG GCT CGG TG	8		
TTT TGA TGG CAG CCA GGG	8		
FAM-CGA CGG TCC GGT TGC TTG GG-Tamra	2		
Cytomegalovirus		US-17	Machida
GCG TGC TTT TTA GCC TCT GCA	20		
AAA AGT TTG TGC CCC AAC GGT A	20		
FAM-TGA TCG GCG TTA TCG CGT TCT TGA TC-Tamra	4		
Epstein-Barr virus		BNRF1 p143	Niesters (2000)
GGA ACC TGG TCA TCC TTT GC	20		
ACG TGC ATG GAC CGG TTA AT	20		
FAM-CGC AGG CAC TCG TAC TGC TCG CT-Tamra	4		
JC virus		minor capsid protein VP3	Aberle unpublished
TGC TCC TCA ATG GAT GTT GC	20		
CAC GGG GTC CTT CCT TTC	20		
FAM-CGG GAC TGT AAC ACC TGC TCT TGA AGC-Tamra	4		

Positive controls or standard samples were used with every run. Commercially available, particle-counted virus standards (Advanced Biotechnologies Inc., Columbia, Md., USA) and standard samples from proficiency panels distributed by the Quality Control for Molecular Diagnostics (QCMD) were used for quantification. Detection limits of PCR were between 100 and 500 copies/ml. Additional numerous negative controls were included in every run. Every positive result was confirmed by a second extraction and amplification.

Qualitative TaqMan real-time PCR

Qualitative real-time PCR was done in the Department of Pathobiology of the Nervous System at the CBR, Vienna. As in the quantitative real-time PCR a TaqMan protocol was applied. 5 µl of DNA were added to the amplification mixture per well, using Sso Fast Probes Supermix (Bio-Rad, Inc., Hercules, CA) for a total volume of 25 µl. Primers and probes were purchased from eurofins MWG Operon.Amplification was performed on CFX Real Time System; C1000 Thermal Cycler (Bio-Rad) with the following cycling conditions: 2' at 95°C followed by 49 cycles of 95°C for 5'' and 55°C for 10'' for examination of CMV cases. In PML cases 45 cycles were performed altogether. Set ups are listed in Tab. 7. Denaturation and annealing temperatures were set as in Prof. Aberle's protocol. Discrepancy concerning durations and extension temperature results from the different master-mix used. C_q was determined by single threshold in all amplifications. Additional negative controls were included.

***Tab. 7**: Real-time PCR set up*

laser-capture	Hsp70^{+} cells (PML pre-experiment)	Hsp40^{+} cells (CMV)	Hsp40^{+} cells (PML
cycles	50	50	45
FAM *)	62.99	45.39	116.28

*) 6-carboxyfluorescein

Statistics

Data were statistically processed and interpreted by GraphPad Prism 6.01. Evaluation was done section-wise. Data group of infected cells with nuclear Hsp70 or Hsp40 immunoreactivity and data group with reactivity in both nucleus and cytoplasm were summed up. Occurrence merely in the cytoplasm was disregarded. Based on these consolidated relative frequencies standard column statistics were carried out; given are average means and standard deviations.

Results

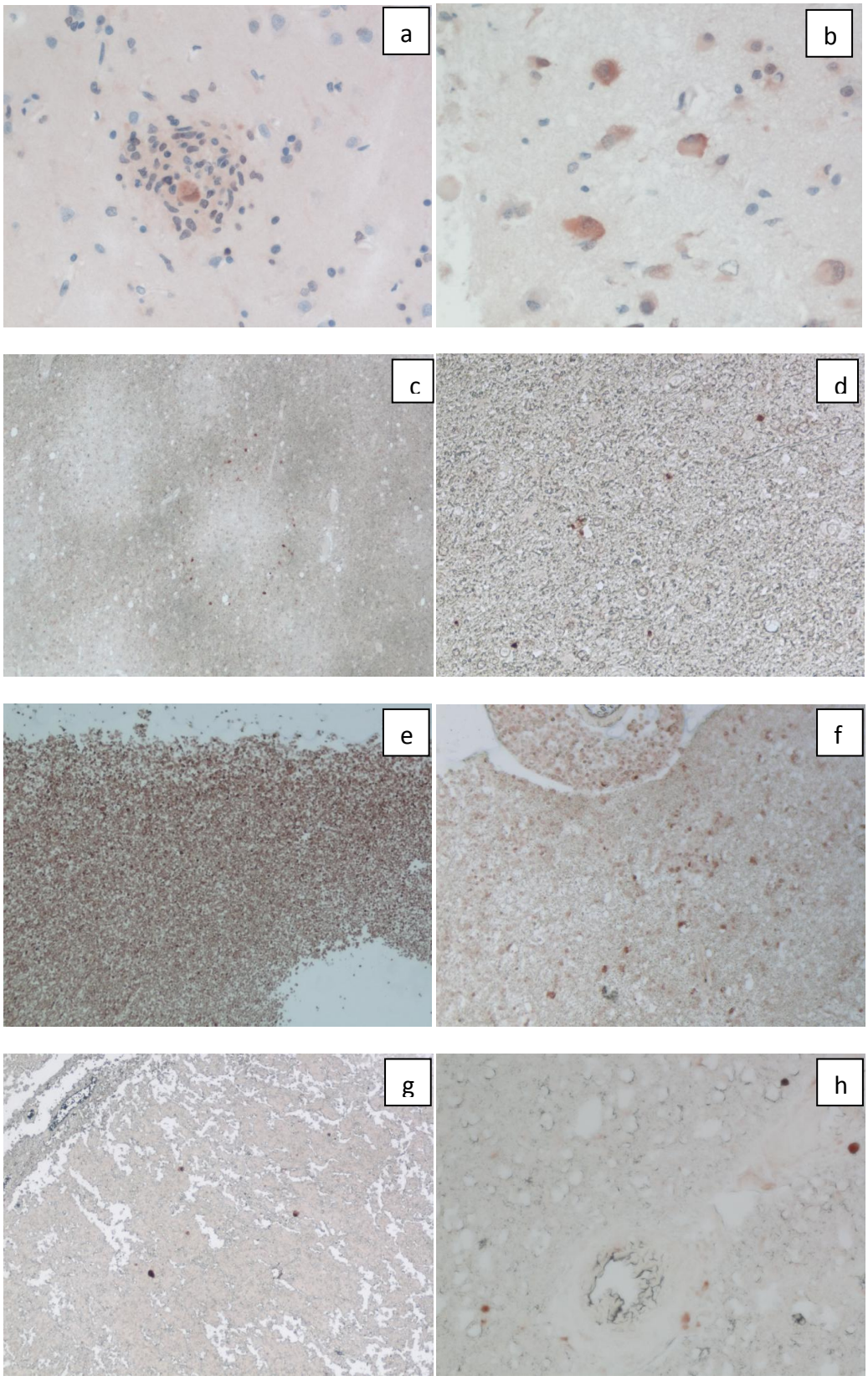

***Fig.3**: Light-microscopy of Hsp40 staining in CMV 234-93-1 (a, b), and of Hsp70 staining in PML 97-93-8 (c) and 214-98-8 (d), EBV 281-00-1 (e), and 130-07-1 (f) as well as in HSV-1 67-83-1 (g), and 204-83-1 (h). a: microglia nodules encircling Hsp40^{+} neuron. b: detail from same lesion. c: Hsp70^{+} cells are visible at the periphery of demyalinated lesions as is typical for location of JC-virus positive glia cells. d: distinct immunoreactivity of α-Hsp70 antibody. e: Hsp70^{+} cells are present throughout the cell culture-based section with nearly no difference in staining intensity. f: despite stronger Hsp70 reactivity in lymphoma autosy material virus marker staining was extremely scattered and not localized to nuclei. g, h: in HSV-1 Hsp70^{+} cells show clear immunoreactivity but also lack to colocalize to virus marker. a - h: all pictures with AEC stainings (in brown).*

1. Immunohistochemistry

Jumping-off thesis was the upregulation and translocation of certain heat-shock proteins as Hsp70 and Hsp40 to the nucleus in virally infected cells as was already shown *in vitro*[22 23] . Basis for this evaluation was immunohistochemical double-labeling using α-Hsp70 and α-Hsp40 antibody combined with respective viral markers.

1. 1. General pathology of virus encephalitis

In CMV encephalitis cases infected cells were present which were found predominantly in periventricular areas as is consistent to literature[24]. One case had severe infection foci with CMV in the cerebellum. Virus marker positive cells prevalently showed an "owl's eyes" phenotype (Fig. 3 b, Fig. 8 j - l). Occurrence of such giant neurons and glial cells represents the typical Cytopathic Effect (CPE) in CMV infections. Regarding white matter pathology inflammation was spreading in most cases and moderate in 62-94-9 and 455-92-7B, edema were observed in 62-94-9 and 234-93-1. Necroses had already developed in 234-93-1 and 559-92-11. Single intranuclear inclusions were also found. Cases 62-94-9 showed uptake of degraded myelin by both microglia and macrophages while in 559-92-11 the myelin remains were removed by macrophages. No white matter pathology was observed in case 290-93-5. In Fig. 8 d - f an oval inclusion is visible where the CMV-specific marker hardly bound but both Hsp70 and To-Pro3 as interkalating ds-DNA detector clearly did so. Fig. 3 a has a microglial nodule encircling a neuron.

Hematoxylin and eosin (HE) and Klüver-Barrera (KLB, a combination of Periodic acid-Schiff and Luxol Fast Blue staining in our case) stain showed that glia cells are infected by the JC virus in PML cases. Although this Polyoma virus only replicates in oligodendrocytes astrocytes are also infected which was visible in larger lesions. Fig. 3 c, d depicts those. Infected oligodendroglial nuclei often appeared enlarged. Concerned astrocytes consistently

showed a special astrogliotic phenotype known as "bizarre astrocytes". Some inclusion-containing nuclei were also present (Fig. 12 d - f, j - l). Progressive loss of myelin sheaths typically occurred at the grey-white junction of the cerebral hemisphere, a phenomenom called "scalloping" in this leukencephalopathy[25]. All cases showed demyelination and spreading inflammation except case 278-93-6 where inflammation was only moderate. Myelin degradation was in an early state throughout with macrophages as scavenging agents.

HSV-1 encephalitis cases exhibited severe inflammation together with neurodegeneration in the central nervous system. Staining for HSV displayed infection of neurons and astrocytes. In HE stains perivascular and meningeal microglial nodules, mononuclear cells, and activated microglia. Demyelination was visible in 67-93-2, 237-91-5, and in 514-82-10. Necrotic tissue was observed in 529-84-6 and in an early state in 330-82-4. Inflammation was moderate in all cases except in 67-83-2 where it appeared heavily.

In EBV both cell cultures and lymphoma EBV was examined. It was not surprising that in cell culture EBV positive cells were vastly present throughout the section. Unfortunately, the *in vivo* infection also showed scattered Hsp70 immunoreactivity unlocalizable to single nuclei. The cause of this phenomemon could not be clarified.

1. 2. Qualitative description of Hsp70 and Hsp40 expression in viral encephalitis cases

CMV

Staining for Hsp70 exhibited the presence of immunoreactivity predominantly in areas with infected cells. Areas without infected cells and without inflammation showed only weak reactivity. Slight occurrence was mostly restricted to the cytoplasm. Double-labeling of Hsp70 with a CMV-specific marker indeed confirmed that nuclear Hsp70 upregulation was seen predominantly in virus-infected cells (Fig. 8). Focal lesions of cells positive for Hsp70 and Hsp40 as well as for virus marker were distinctly visible. Hsp40, one of the main interaction proteins of Hsp70, to a large degree displayed similar staining. Both heat-shock proteins showed comparable patterns in both upregulation and nuclear translocation as was shown in 4 out of 6 examined CMV cases. In 2 cases no viral marker reactivity was found (Tab. 15, Fig. 6). A higher portion of virus marker positive cells showed cytoplasmatic localization of Hsp40 than Hsp70. Ratio of nuclear colocalization was nearly identical. In many cells nuclear Hsp70 staining was observable in enlarged neurons and glial cells with only little or no cytoplasmatic immunoreactivity. This reactivity frequently appeared blotchy and left nuclear parts unstained. Fig. 8 d - f shows a virus marker positive nucleus with almost no Hsp70 staining visible except for the elongate discontinuous area at the rim where in contrast virus marker reactivity is very weak. To-Pro3 iodide staining for the display of

dsDNA is also intense in this intranuclear region. Hsp40 staining (Fig. 8 g - l) in enlarged neurons appeared blotchy with unstained intranuclear areas and lighter intensity outreaching to the cytoplasm.

PML

Labeling for Hsp70 showed strongly stained immunoreactive cells at the periphery of demyelinating lesions. In PML cases, a clear upregulation of Hsp70 and Hsp40 in oligodendrocytes was found that was present in the nuclei in many cases as was expected for a DNA virus (Fig. 9, Fig. 10). Astrocytes were affected to a lesser extent, predominantly to those showing bizarre phenotype. The data showed a higher ratio of cells positive for both virus marker α-SV40 antibody and Hsp40 than for the respective colocalization with Hsp70. Moreover, very little cells showed no virus marker and Hsp40 colocalization while these portion in Hsp70 stainings was about 10 times higher. Virus-infected oligodendrocytes sometimes showed additional strong cytoplasmatic expression but also strong and clear translocation of Hsp70 and Hsp40 into their nucleus. This depended on the region. Nuclear Hsp70 reactivity was typically visible in virus marker positive cells while cells outside virally infected areas showed upregulation of this chaperone in the cytoplasm only. This upregulation was comparatively weaker than in virus marker positive cells. Staining in nuclei appeared dot-wise at the rim of the nucleus with more intensive fluorescence intensity in some but not all cases as described by Burch and Weller (Fig. 12 b). Adjacent virus marker positive inclusion bodies were found there (Fig. 12 d - f). In other cells staining of Hsp70 was present throughout the nuclei. Both occurrences were observable in the Hsp40 stainings as well (Fig. 12 g - l).

HSV-1

In contrast to *in vitro* studies mentioned above[8 9] no acceptable colocalization of Hsp70 or Hsp40 positive cellus and cells positive for the HSV-specific virus marker were detectable. Both populations were scattered throughout the sections. In addition, cells with upregulated Hsp70 (Fig. 13) did not display nuclear translocation of the heat-shock proteins of interest therefore lacking an important criterion. Various immunohistochemical staining protocols failed to deliver usable findings in HSV-1 material. Hsp40 stainings were also prepared but could not show colocalization either.

EBV

Colocalization of both Hsp70 and viral marker reactivity was even lower than in the HSV-1 samples. Neither encephalitic material from a lymphoma patient nor cell cultured EBV delivered noticeable results. Hsp40 stainings were also prepared but did no display visible colocalization.

HIV, SSPE (Measles virus), and TBE

Neither colocalization of Hsp70 nor Hsp40 and viral marker reactivity was visible in cases containing the complex retrovirus HIV. ss(+)RNA Measles virus infection of Subacute Sclerotizing Panencephalititis (SSPE) patients did not display colocalization of Hsp40 and virus marker reactivity, neither. This also was the case with TBE material ss(-)RNA virus TBE. Despite pretreatment variations it was not possible to establish suitable double-staining procedures. Respective antigens in HIV, SSPE, and TBE were displayed light-microscopically.

1. 3. Quantitative evaluation of Hsp70 and Hsp40 localisation in infected cells

Aim of the work was to evaluate the capability of Hsp70 and Hsp40 to display virally infected cells without utilization of a virus marker. In order to assess the localisation of Hsp70 and Hsp40 reactivity in virus-infected cells we quantified the presence of these chaperones in the nucleus and/or in the cytoplasm of those cells. To achieve maximum selectivity only cells with nuclear Hsp70 or Hsp40 reactivity occurring were taken into account. The number of virus marker positive cells with only cytoplasmatically upregulated Hsp70 or Hsp40 was very low. An explanation may be the tried and tested staining conditions, especially regarding antigen retrieval and antibody concentrations, acquired in numerous pre-experiments.

Hsp70 reactivity

Tab. 8 gives a survey of the evaluated sections in relative frequencies of nuclearly translocated and upregulated Hsp70 (Fig. 4). Colocalization means of the single sections ranged from 1.6 % in EBV (labeled by α-EBV zebra antibody) up to 78.9 % in CMV. Standard deviations values are in accordance with histological analyses. For details of respective virus encephalitides see following sections below. Depiction of fig. 4 contrasts the nuclear reactivity of Hsp70 in the different diseases. Average colocalization mean in CMV is 45.8 % and 47.9 % and 45.5 %, respectively, in PML, depending on the applied antibody. In HSV-1 colocalization ratio is only 16.1 % and 4.3 % and 1.6, respectively, in EBV, again depending on the used antibody.

***Tab. 8**: Overview on relative frequencies of virus-marked cells with nuclear Hsp70 reactivity per case in evaluated encephalitides*

cases	CMV	PML SV40	PML PAb2003	HSV	EBV LMP	EBV zebra
1	13.0	59.8	61.3	0	8.0	1.5
2	78.9	13.3	61.3	0	0.6	1.6
3	47.8	6.0	28.1	0.8		
4	43.3	65.9	36.6	5.4		
5		73.5	53.8	47.8		
6		50.0	31.9	42.3		
7		66.9				

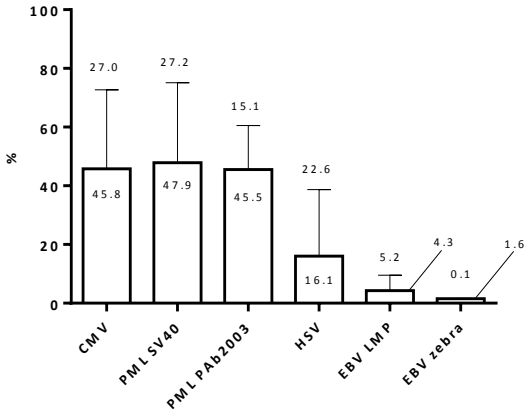

***Fig. 4**: Graphical representation of nuclear Hsp70 reactivity evaluation in CMV (n = 4), PML (n = 7, and 6, resp.), HSV-1 (n = 6), and EBV (n = 2, and 2, resp.); Y-axis depicting percentage of infected cells; figure inside columns or indicated by line = mean, figure above error bars = standard deviation*

Hsp40 reactivity

CMV and PML cases were also applied α-Hsp40 antibody to evaluate the colocalization fraction of virally marked cells and co-chaperone Hsp40. Polyclonal α-Hsp40 antibody was used. CMV and PML samples were taken as previous analyses on Hsp70 yielded feasible results. Hsp40 reactivity showed similar outcome as Hsp70 findings and even exceeded these. In Tab. 9 an overview of the single sections of both virus infections is listed. In CMV average mean was 56.2 % while in PML labeled by α-SV40 antibody this value even was 94.6 % with a standard deviation of only 2.9 (Fig. 5). Hsp40 seems to be an excellent marker for JC virus infected cells in vivo. For details of the different encephalitides also see respective sections below.

***Tab. 9**: Overview on relative frequencies of virus-marked cells with nuclear Hsp40 reactivity per case in evaluated encephalitides*

cases	CMV	PML SV40
1	76.9	94.7
2	67.7	96.4
3	56.5	97.2
4	23.7	91.2
5		91.7
6		98.6
7		92.4

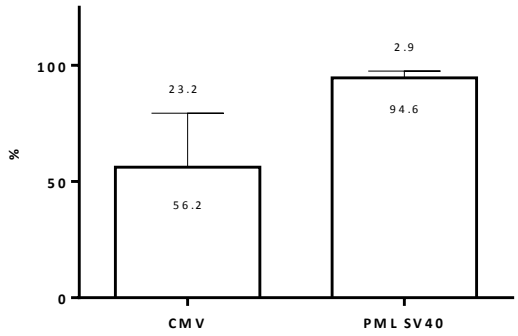

***Fig. 5**: Graphical representation of nuclear Hsp40 reactivity evaluation in CMV (n = 4) and PML (n = 7); Y-axis depicting percentage of infected cells; figure inside columns = mean, figure above error bars = standard deviation*

CMV

Hsp70 reactivity

Polyclonal Hsp70 antibody had to be used for CMV cases. Tab. 10 shows the cellular location of upregulated Hsp70 with the main statistical parameters in Fig. 6. A nuclear immunohistochemical Hsp70 signal was visible in an average of 27.1 % of cases, while 18.4 % had Hsp70 reactivity in this cell compartment and also in the cytoplasm. Both values sum up to 45.5 %. Only averaged 3.7 % of virus marker positive cells exhibited an Hsp70 signal merely in the cytoplasm. 50.8 % of the cells on average displayed no Hsp70 reactivity at all. In 2 out of 6 sections (290-93-5 and 430-93-7) no virus positive cells were found leading to 4 examinable cases (Tab. 10). In Fig. 6 exemplary pictures from confocal fluorescence microscopy are found.

***Tab. 10**: Location and relative frequencies of Hsp70 reactivity in virus-marked cells in CMV cases*

	Hsp70$^+$			
	nuclear	nuclear and cyt.	cyt.	none
62-94-9	6.5	6.5	0.0	87.0
234-93-1	47.4	31.6	10.5	10.5
455-92-7B	34.8	13.0	4.3	47.8
559-92-11	19.7	22.5	0.0	57.7

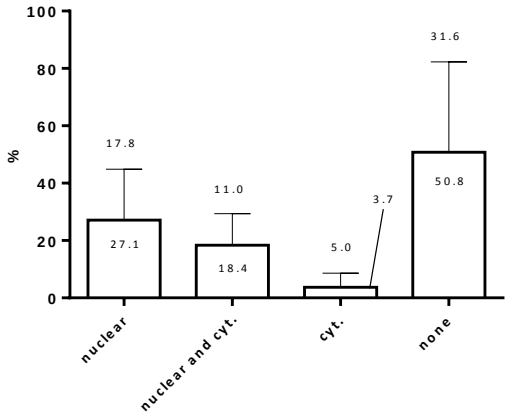

***Fig. 6**: Graphical representation of Hsp70 reactivity evaluation in CMV (n = 4); Y-axis depicting percentage of infected cells; figure inside columns or indicated by line = mean, figure above error bars = standard deviation*

Hsp40 reactivity

Hsp40 was also applied to CMV sections as the Hsp70 colocalizations showed feasible results. In a mean of 27.7 % of cases Hsp40 was found upregulated and translocated to the nucleus and in an additional 28.5 % also in the cytoplasm giving a sum of 56.2 % (Fig. 7). In only 4.3 % of cases Hsp40 reactivity was only visible in the cytoplasm. Locations and relative frequencies of Hsp40 immunoreactivity are quoted in Tab. 11. Fig. 7 contains a graphical depiction of these subcellular localizations. Various examples of fluorescent microscopical impressions of colocalizations are found in Fig. 8.

***Tab. 11**: Location and relative frequencies of Hsp40 reactivity in virus-marked cells in CMV cases*

	Hsp40$^+$			
	nuclear	nuclear and cyt.	cyt.	none
62-94-9	38.5	38.5	0.0	23.1
234-93-1	14.5	53.2	12.9	19.4
455-92-7B	54.3	2.2	0.0	43.5
559-92-11	3.6	20.1	4.3	71.9

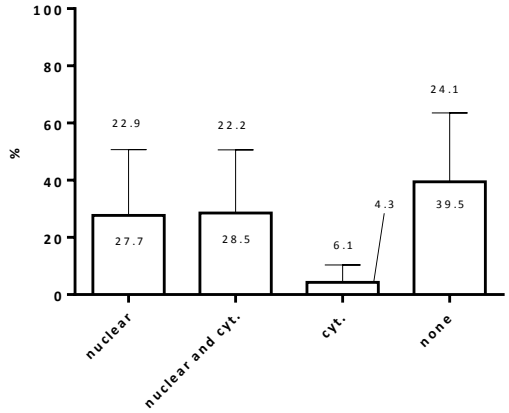

***Fig. 7**: Graphical representation of Hsp40 reactivity evaluation in CMV (n= 4); Y-axis depicting percentage of infected cells; figure inside columns or indicated by line = mean, figure above error bars = standard deviation*

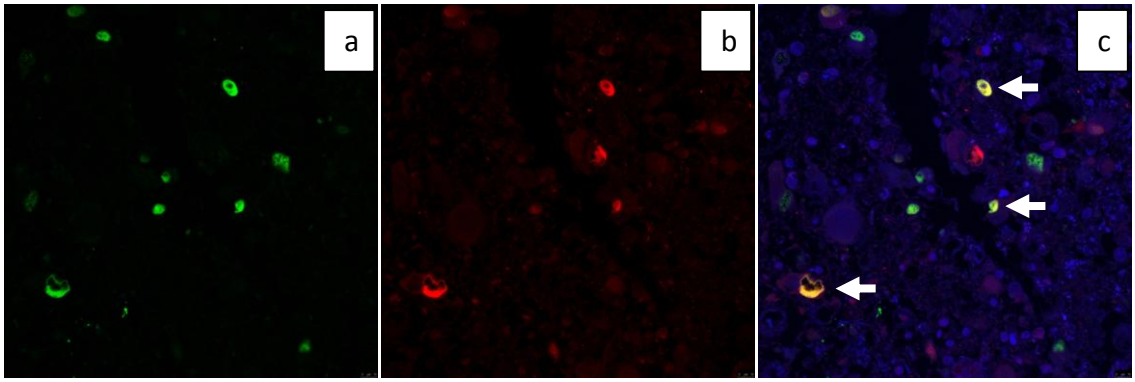

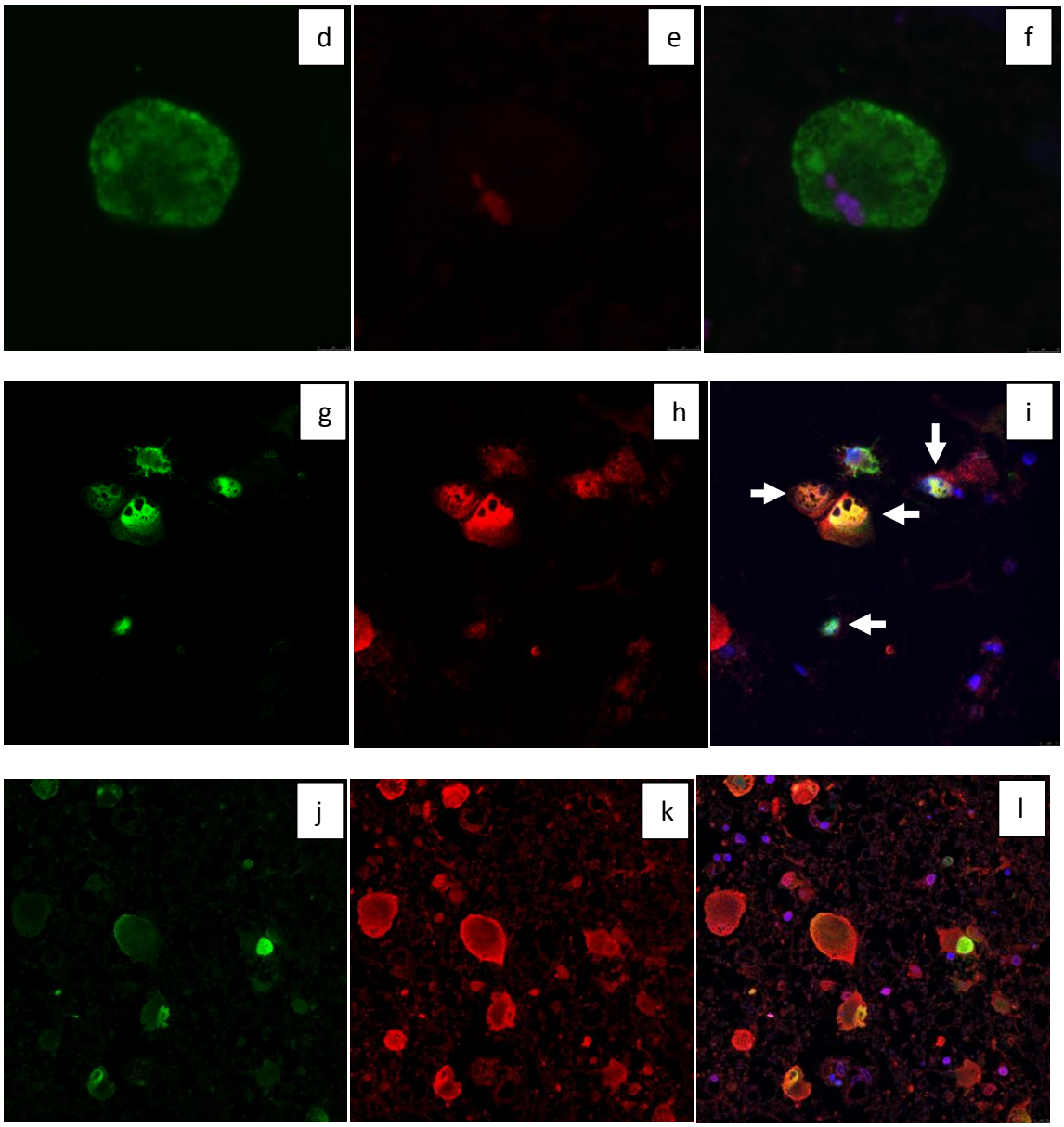

Fig. 8*: Confocal laser microscopy of Hsp70 and Hsp40 colocalizations in CMV. a - f: Hsp70 labeling in case 455-92-7B. a - c: nuclei stained with monoclonal α-CMV antibody. b: staining with polyclonal α-Hsp70 antibody. c: channels merged, colocalizations in yellow (arrows). d - f: single nucleus further magnified, staining as in pictures above. Readily distinguishable is the elongate region in the lower part of the nucleus showing reduced virus marker reactivity but high DNA concentration according to To-Pro3 staining and Hsp70 reactivity. g - l: Hsp40 labeling in cases 234-93-1 (g - i) and 455-92-7B (j - l). 234-93-1. g: nuclei stained with monoclonal α-CMV antibody. h: staining with polyclonal α-Hsp40 antibody. i: all channels merged, colocalizations in yellow (arrows). j: Owl's eyes, a typical Cytopathic Effect in CMV infection. k: staining with polyclonal α-Hsp40 antibody shows colocalized heat-shock protein. l: all channels merged, colocalizations indicated by arrows. c, f, i, l: overlay includes To-Pro3 nuclei staining appearing in blue.*

PML

Hsp70 reactivity

Trigger of PML is the JC virus against which two different antibodies (α-SV40 large T antigen and α-Pab 2003 antibody) were available. Both antibodies gave similar results. Seven sections were analyzed. Because of the monoclonal character of the α-SV40 virus marker antibody the use of monoclonal α-Hsp70 antibody was feasible. The means of colocalization of both Hsp70 and this virus marker range from 5.4 % to 73.5 %. This results to an average of 43.1 % (SD = 26.4) (Fig. 9). Cellular location of Hsp70 upregulation was the nucleus in 43.1 % of cases together with 4.8 % co-occcurrence in the cytoplasm (Fig. 9). In no case Hsp70 was present only in the cytoplasm except in 359-93-7A2 where 2.8 % of cells showed this phenotype. This case exhibited a mean average of 33.1 % of cells showing Hsp70 also in the cytoplasm. Nearly all of the other α-SV40 antibody marked cells of PML patients displayed only nuclearly translocated Hsp70. An average of 51.7 % virus marker positive cells occurred without conspicuous Hsp70 reactivity. Second antibody that was used for evaluation of Hsp70 and JC virus marker colocalizations in PML was the monoclonal α-PAb2003 antibody. Roughly as with α-SV40 antibody stainings, fraction of virus marker stained cells displaying translocated Hsp70 into the nucleus was 43.6 % on average (Tab. 14). Fig. 11 contrasts the cellular location of conspicuous Hsp70. 1.9 % also showed this protein in upregulated form in the cytoplasm and 0.3 % only there. 54.3 % had no Hsp70 reactivity compared to 51.7 % in the α-SV40 stained sections. Analysis of case 103-93-8 was erroneously left out, so that six sections were evaluated with this antibody. Compared to α-SV40 antibody double-stainings with Hsp70 appeared with less background in α-PAb2003 cases. Exemplary fluorescence pictures are in Fig. 12.

***Tab. 12**: Location and relative frequencies of Hsp70 reactivity in virus-marked cells in PML cases (by α-SV40 antibody)*

	Hsp70$^+$			
	nuclear	nuclear and cyt.	cyt.	none
12-93-2	59.8	0.0	0.0	40.2
97-93-8	13.3	0.0	0.0	86.7
47-93-3	5.4	0.5	0.0	94.0
103-93-8	65.9	0.0	0.0	34.1
278-93-6	73.5	0.0	0.0	26.5
358-93-6	50.0	0.0	0.0	50.0
359-93-7A2	33.8	33.1	2.8	30.3

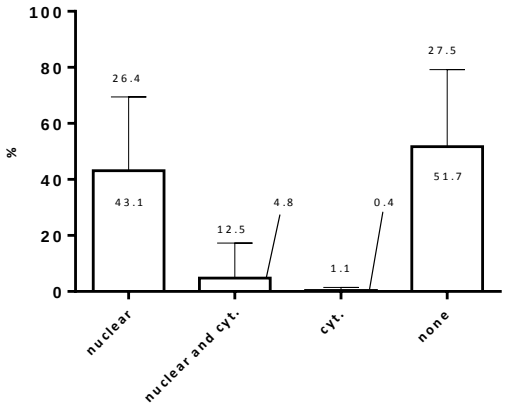

Fig. 9*: Graphical representation of Hsp70 reactivity evaluation in PML cases (by α-SV40 antibody, n = 7) ; Y-axis depicting percentage of infected cells; figure inside columns or indicated by line = mean, figure above error bars = standard deviation*

Hsp40 reactivity

Hsp40 colocalization ratios were even higher than in labelings by α-Hsp70 antibody which may be influenced by the polyclonal character of the first (Tab. 13, Fig. 10). An average mean of 73.9 % of α-SV40 antibody marked cells showed translocation to the nucleus with a relatively low standard deviation of 5.2. Together with the fraction of Hsp40 appearing in both nucleus and cytoplasm this means a colocalization of 94.6 %. Only 0.6 % of cells appeared with cytoplasmatic Hsp40 reactivity. 4.8 % of virus marker positive cells did not show any upregulation of Hsp40.

Tab. 13*: Location and relative frequencies of Hsp40 reactivity in virus-marked cells in PML cases (by α-SV40 antibody)*

	Hsp40$^+$			
	nuclear	nuclear and cyt.	cyt.	none
12-93-2	82.1	12.6	0.0	5.3
47-93-3	68.9	27.6	0.0	3.6
97-93-8	71.8	25.4	0.0	2.8
103-93-8	67.9	23.3	4.4	4.4
278-93-6	77.7	14.0	0.0	8.3
358-93-6	71.5	27.1	0.0	1.4
359-93-7A2	77.3	15.2	0.0	7.6

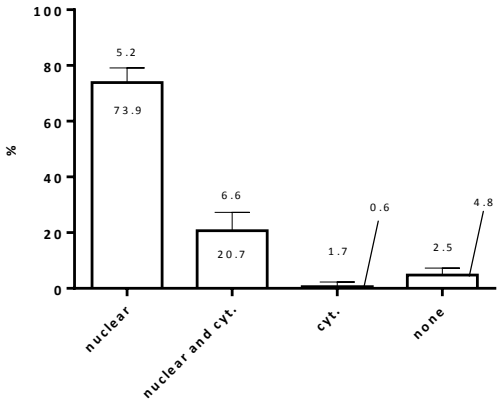

Fig. 10*: Graphical representation of Hsp40 reactivity evaluation in PML cases (by α-SV40 antibody, n = 7) ; Y-axis depicting percentage of infected cells; figure inside columns or indicated by line = mean, figure above error bars = standard deviation*

Tab. 14*: Location and relative frequencies of Hsp70 reactivity in virus-marked cells in PML cases (by α-PAb2003 antibody)*

	Hsp70$^+$			
	nuclear	nuclear and cyt.	cyt.	none
12-93-2	61.3	0.0	0.0	38.7
97-93-8	59.7	1.6	0.0	38.7
47-93-3	28.1	0.0	1.5	70.4
278-93-6	34.1	2.4	0.0	63.4
358-93-6	53.8	0.0	0.0	46.2
359-93-7A2	24.8	7.1	0.0	68.1

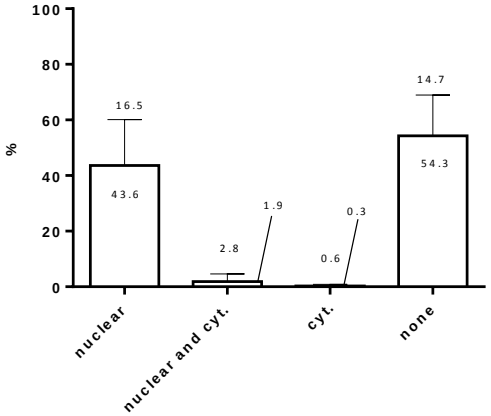

Fig. 11*: Graphical representation of Hsp70 reactivity evaluation in PML cases (by α-PAb2003 antibody, n = 6) ; Y-axis depicting percentage of infected cells; figure inside columns or indicated by line = mean, figure above error bars = standard deviation*

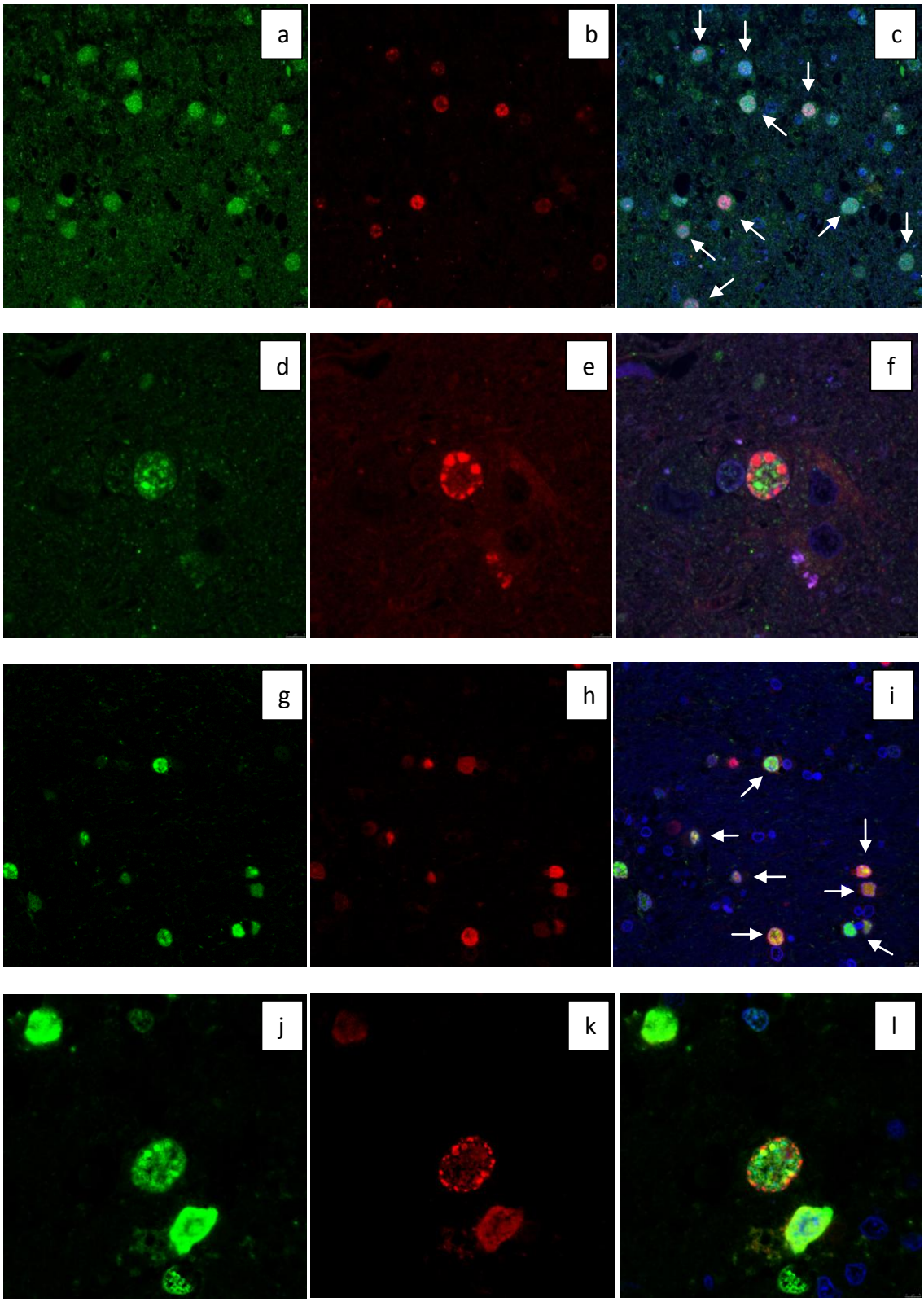
a
b
c
d
e
f
g
h
i
j
k
l

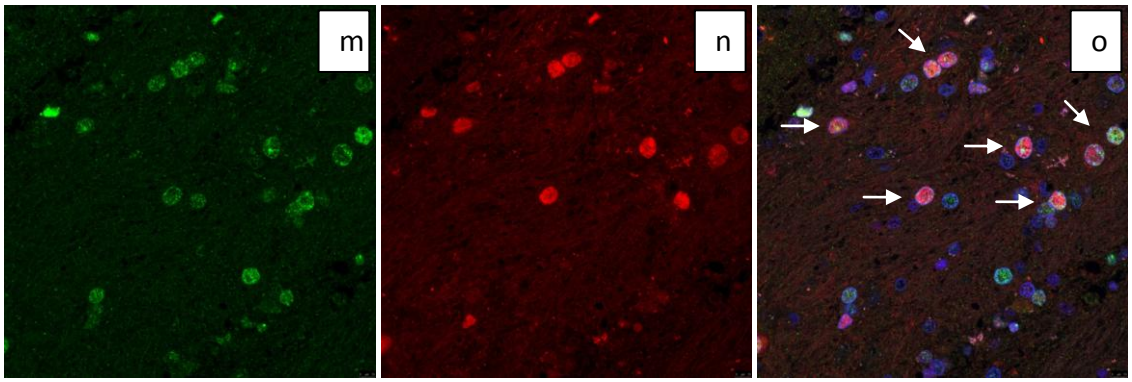

***Fig. 12**: Confocal laser microscopy of Hsp70 or Hsp40 colocalizations in PML. a – l: virus marker labeling by α-SV40 large T antigen antibody. a - f: Hsp70 labeling in case 97-93-8. a - c: cells stained with plyclonal α-SV40 antibody. b: staining with monoclonal α-Hsp70 antibody. c: channels merged, colocalizations indicated by arrows. d - f: single α-SV40 reactive nucleus further magnified. d: Inclusion bodies in α-SV40 reactive nucleus. e: neighboring Hsp70 reactivity indicating to intranuclear regions of viral DNA replication or viral protein assembly. f: Channels overlaid. c, f: overlay includes To-Pro3 nuclei staining appearing in blue. g - l: Hsp40 labeling in cases 359-93-7A2 (g - i) and 47-93-3 (j - l). g: polyclonal α-SV40 antibody. h: polyclonal α-Hsp40 antibody. i: channels merged. j: inclusion bodies in α-SV40 reactive nucleus. k: neighboring Hsp40 reactivity indicating to intranuclear regions of viral DNA replication or viral protein assembly. l: Channels merged.m - o: virus marker labeling by α-PAb2003 antibody in case 12-93-2. m: monoclonal α-PAb2003 antibody. n: polyclonal α-Hsp70 antibody. o: channels merged. c, f, i, l, o: overlay includes To-Pro3 nuclei staining appearing in blue.*

HSV-1

Hsp70 reactivity

Although *in vitro* experiments in principal showed a coincidence of upregulated Hsp70 transported to the nucleus in HSV-1$^+$ cells our evaluation failed to do so (Tab. 15, Fig. 13). Despite various pre-experiments with different pretreatment processes and antibody concentrations distinct colocalizations were not detectable. An averaged mean of 83.2 % of virally marked cells did not exhibit Hsp70 reactivity. 9.1 % showed a nuclear signal. The rest is alotted to both nuclear and cytoplasmatic occurrence of Hsp70 (7.0 %) or was visible only in the cytoplasm (0.7 %). 16.1 % of HSV-1-infected cells display upregulated and nucleus-translocated Hsp70. For the six cases monoclonal Hsp70 antibody was used. Exemplary pictures of colocalizations in nuclei are visible in Fig. 14 a - c. As an alternative, light-microscopic detection of colocalizations on separate sections was tried but failed to exhibit colocalizations (Fig. 14 d, e).

***Tab. 15**: Location and relative frequencies of Hsp70 reactivity in virus-marked cells in HSV-1 cases*

	Hsp70$^+$			
	nuclear	nuclear and cyt.	cyt.	none
67-83-2	0.0	0.0	0.0	100.0
204-83-4	0.0	0.0	0.0	100.0
237-91-5	0.0	0.8	0.0	99.2
330-82-4	0.0	5.4	0.0	94.6
455-92-7B	34.8	13.0	4.3	47.8
559-92-11	19.7	22.5	0.0	57.7

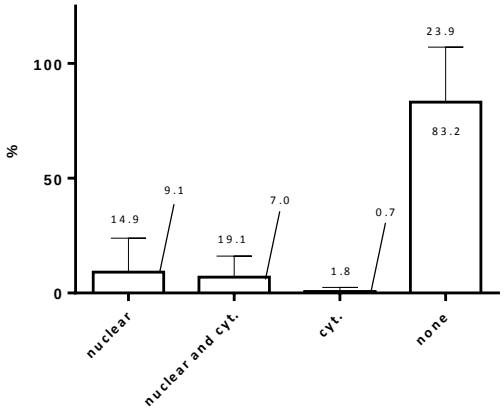

***Fig. 13**: Graphical representation of Hsp70 reactivity evaluation in HSV-1 (n = 6); Y-axis depicting percentage of infected cells; figure inside columns or indicated by line = mean, figure above error bars = standard deviation*

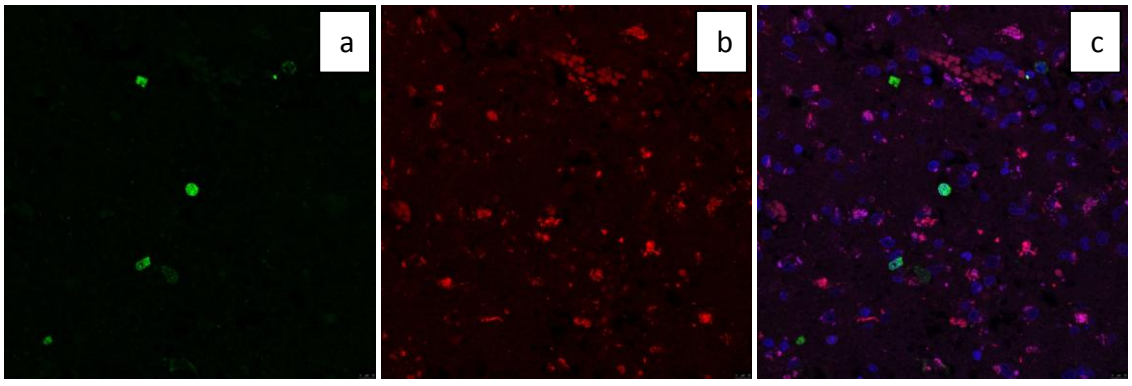

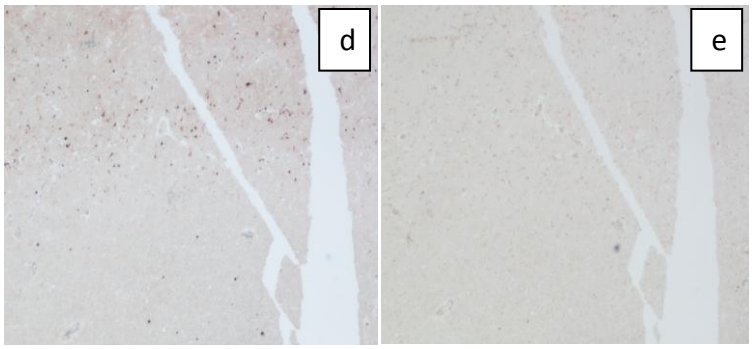

Fig. 14*: a – c: confocal laser microscopy of Hsp70 colocalizations in HSV-1 case 237-91-5. a: labeling by polyclonal α-HSV antibody. b: scattered reactivity of monoclonal α-Hsp70 antibody. c: in the overlay of the channels no colocalizations of virus marker and Hsp70 is visible, merged depiction includes To-Pro3 nuclei staining appearing in blue. d, e: light-microscopic assessment of colocalizations of HSV-1 infected and Hsp70^{+} cells on separate sections of case 237-91-5, magnification 40x. d: polyclonal α-HSV antibod. e: monoclonal α-Hsp70. magnification 40x.*

EBV

Hsp70 reactivity

Also available was one section of Epstein-Barr virus autopsy material from a lymphoma patient and one from EBV cell cultures. In both cases, no colocalizations of virus marker and Hsp70 was visible. Two different antibodies were applied. First, monoclonal α-EBV LMP was tested, combined with a polyclonal α-Hsp70 antibody. A mean average of 95.7 % of EBV LMP positive nuclei did not exhibit Hsp70 reactivity. 3.8 % showed Hsp70 in the nucleus and a further fraction of 0.6 % also cytoplasmatically. Cytoplasmatic reactivity only was observed in no case (Tab. 16, Fig. 15). The second EBV antibody we used was α-EBV zebra antibody. Results were similar to α-EBV LMP antibody. The colocalization fraction of virally marked cells and nuclear Hsp70 reactivity was 1.2 %, actually less than with α-EBV LMP. 0.4 % of nuclei exhibited this protein also in the cytoplasm (Tab. 17, Fig. 16). As with the α-EBV LMP antibody no cytoplasmatic immunoreactivity was detectable. Some of this little colocalization portion showing nuclei are visible in Fig. 17. The fig. shows fluorescence microscopy pictures from Hsp70 reactivity assessments in EBV lymphoma case 130-07-1. The small colocalization ratio in EBV cases might be due to technical problems like intense background staining, as it was observed especially in cell cultured sample 281-00-1. Less antibody concentration or reduced pre-treatment could deliver a solution to these problems. We would therefore not exclude the possibility that Hsp70 and Hsp40 could act as virus markers in EBV, too.

***Tab. 16**: Location and relative frequencies of Hsp70 reactivity in virus-marked cells in EBV cases (by α-LMP antibody)*

	Hsp70$^+$			
	nuclear	nuclear and cyt.	cyt.	none
281-00-1 LMP	6.9	1.1	0.0	92.0
130-07-1 LMP	0.6	0.0	0.0	99.4

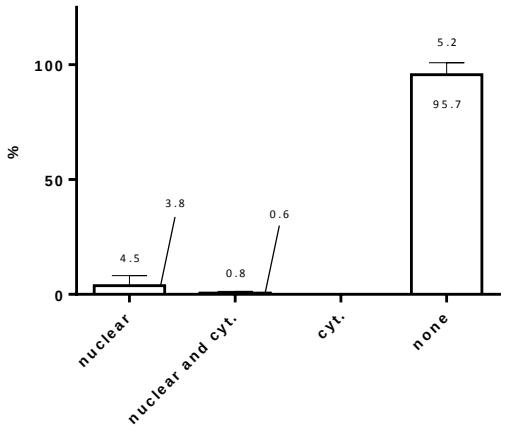

***Fig. 15**: Graphical representation of Hsp70 reactivity evaluation in EBV (n = 2); Y-axis depicting percentage of infected cells; figure inside columns or indicated by line = mean, figure above error bars = standard deviation*

***Tab. 17**: Location and relative frequencies of Hsp70 reactivity in virus-marked cells in EBV cases (by α-EBV zebra antibody)*

	Hsp70$^+$			
	nuclear	nuclear and cyt.	cyt.	none
281-00-1 zebra	0.8	0.8	0.0	98.5
130-07-1 zebra	1.6	0.0	0.0	98.4

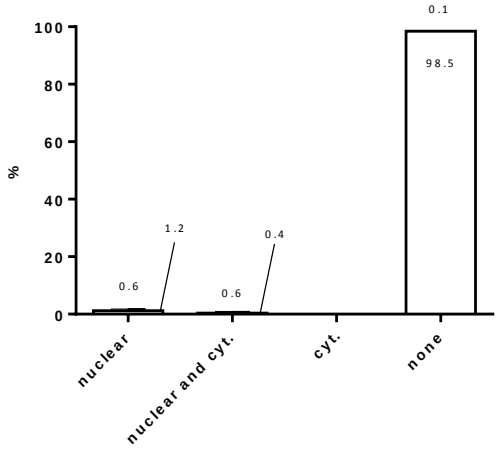

***Fig. 16**: Graphical representation of Hsp70 reactivity evaluation in EBV (n = 2); Y-axis depicting percentage of infected cells; figure inside columns or indicated by line = mean, figure above error bars = standard deviation*

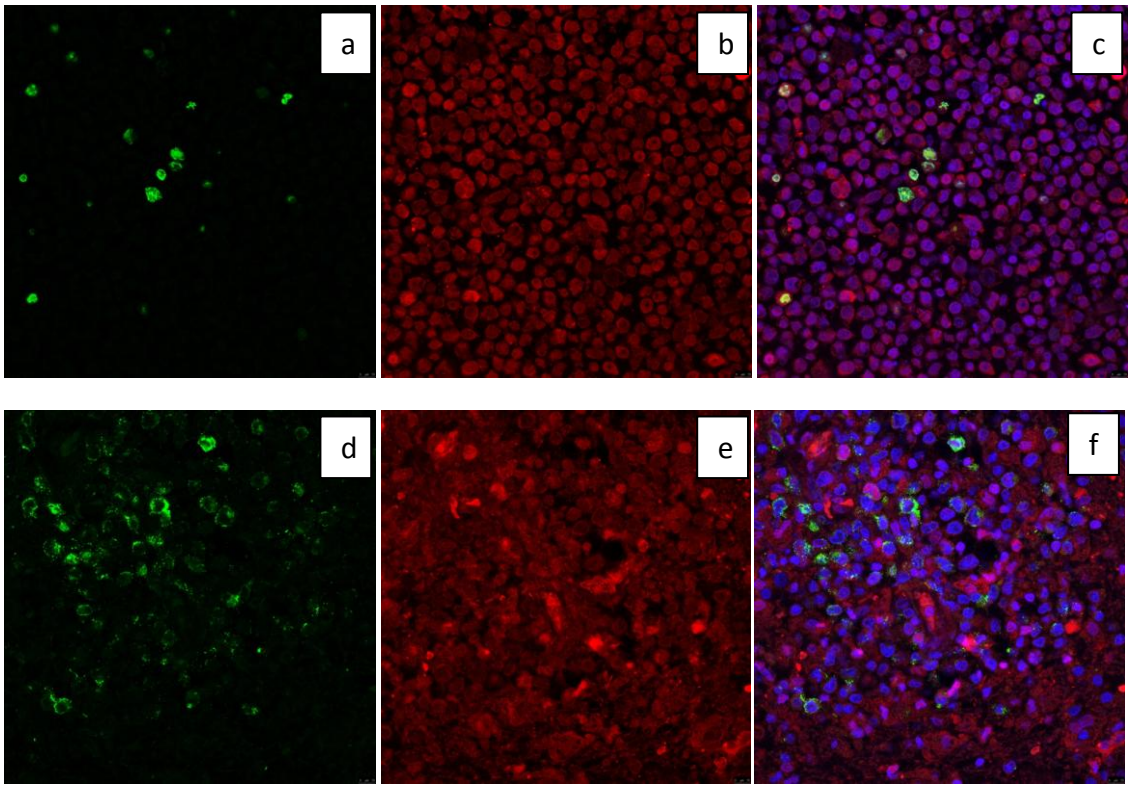

***Fig. 17**: Confocal laser microscopy of Hsp70 colocalizations in EBV. a - c: EBV cell culture (case 281-00-1). a: nuclei stained with virus marker α-EBV zebra antibody. b: polyclonal α-Hsp70 antibody, intense background staining. c: channels merged, some colocalizations visible. d - f: lymphoma EBV in case 130-07-1. d: monoclonal α-EBV LMP antibody appeared scattered throughout section of lymphomatic material. e: polyclonal α-Hsp70 antibody. f: in the overlay depiction nearly no colocalizations were detectable. c, f: merged depiction includes To-Pro3 nuclei staining appearing in blue.*

2. Genetics: detection of viral DNA in Hsp70$^+$ and Hsp40$^+$ cells by real-time PCR

Goal of these studies was to find out whether Hsp70 or Hsp40 can be used as markers to identify virus-infected cells. In this part of the study we tested whether we could trace viral DNA of known viruses after staining and concurrent isolation of DNA from Hsp70 or Hsp40 positive nuclei.

2.1. Detection of viral DNA in immunohistochemically untreated sections

In a first step DNA was isolated from paraffined sections from immunohistochemically untreated sections. Isolated DNA was subjected to quantification by TaqMan real-time PCR. The results show that in these complete sections viral DNA indeed could be retrieved. However, positive identification of viral DNA could only be shown in PML (n = 3) and EBV cases (n = 1). No identification of viral DNA was possible in CMV cases (n = 2), see Tab. 20. Paraffined CMV and PML sections as well as paraffined Epstein-Barr virus (human herpesvirus 4 = HHV-4) infected cells from cultures and HHV-6 infected cells from cultures were scratched off glass slides on the whole by a throw-away scalpel. DNA was extracted for quality analysis by PCR using β-actin specific primers. Aim was to ensure adequate DNA integrity. The large ratio of photospectrometrically determined DNA concentrations presumably falls upon human DNA and only secondary upon viral DNA (Tab. 18). DNA concentrations were relatively low and ranged from 4.6 ng/µl in HSV-1 sample 529-84-6 to 24.9 ng/µl in PML sample 97-93-8. 260/280 sample purity ratios of ≈ 1.8 usually are accepted as "pure" for DNA. Most values are found around this value. Lower values as in HHV-6 sample 278-00 can point to protein, phenol or other contaminations that strongly absorb at or near 280 nm. 260/230 ratio as a second measure for sample purity should commonly be in the range of 2.0 – 2.2. As numerous values are lower contaminants absorbing at or near 230 nm could be present. Small changes in pH are also known to influence sample purity ratios in photospectroscopy. For HHV-6 sample 278-00 originated from cell cultures material from two sections was pooled. Also cell cultured origin had EBV 281-00-1.

***Tab. 18**: Photospectrometric determination of DNA concentrations of IHC untreated samples; DNA concentration is given in ng/µl. Measurement were performed by using a NanoDrop2000 spectrometer as described in "Material and Methods".*

CMV	**DNA conc.**	**A260 (RNA)**	**A280 (protein)**	**260/280 (sample purity)**	**260/230 (sample purity)**
290-93-5	9.2	0.185	0.104	1.77	1.51
234-93-9	8.7	0.173	0.102	1.69	2.75
430-93-6	8.6	0.171	0.103	1.67	1.57
118-94-1	20.7	0.414	0.236	1.75	1.78
PML					
214-98-8	12.9	0.259	0.138	1.88	0.97
471-93-6	14.2	0.283	0.157	1.81	1.82
342-93-5	10.8	0.217	0.126	1.72	1.56
97-93-8	24.9	0.499	0.282	1.77	1.84
HHV-6					
278-00	5.1	0.101	0.078	1.3	0.89
EBV					
281-00-1	6.4	0.127	0.081	1.57	0.73
HSV-1					
67-83-2	4.8	0.096	0.048	1.95	1.86
204-83-1	17.5	0.350	0.244	1.44	0.84
237-91-5	6.9	0.139	0.082	1.76	2.14
330-82-4	5.2	0.105	0.052	2.00	3.08
514-82-10	6.8	0.135	0.085	1.58	1.11
529-84-6	4.6	0.893	0.049	1.89	2.65

Extracted DNA was PCR amplified with β-actin specific primers. EBV 281-00-1, CMV 430-93-6 and 118-94-1 as well as PML 214-98-8, 342-93-5, and 97-93-8 showed positive results. No bands were detected for the remaining samples. Possibly, the degree of DNA fragmentation in this cases was too high due to fixation and paraffin embedding treatment. Most of the sections were 18 to 19 years old at time of analysis. As positive control new material from an RE case received this year (Y304-12) was used therefore. In contrast to the autopsy material in the other encephalitides this RE material came from surgigal excision followed by immediate fixation. Actin bands were visible for the EBV section, for 2 out of 4 CMV sections, and for 3 out of 4 PML sections as well as for the RE positive control (Fig. 18). All positive samples were further assessed by real time-PCR. Although repeatedly tried, CMV samples did not show positive results in real-time PCR by virus-specific primers. All 3 PML samples as well as the EBV sample yielded positive results. Quantification of copy numbers (Tab. 20) appeared in a wide range and appeared without consistency. While cell-cultured EBV sample 281-00-1 contained 1.3 x 10^5 copies it was 4.2 x 10^5 in the *in vivo* preparations, thus nearly 3 times more. PML copies stained had 2.2 x 10^5, and 1.7 x 10^5 copies (1.7 x 10^4 and 7.4 x 10^5 unstained). HSV-1 copies were 1.1 x 10^3, and 1.9 x 10^5 copies (2.4 x 10^4 and 1.3 x 10^7 unstained).

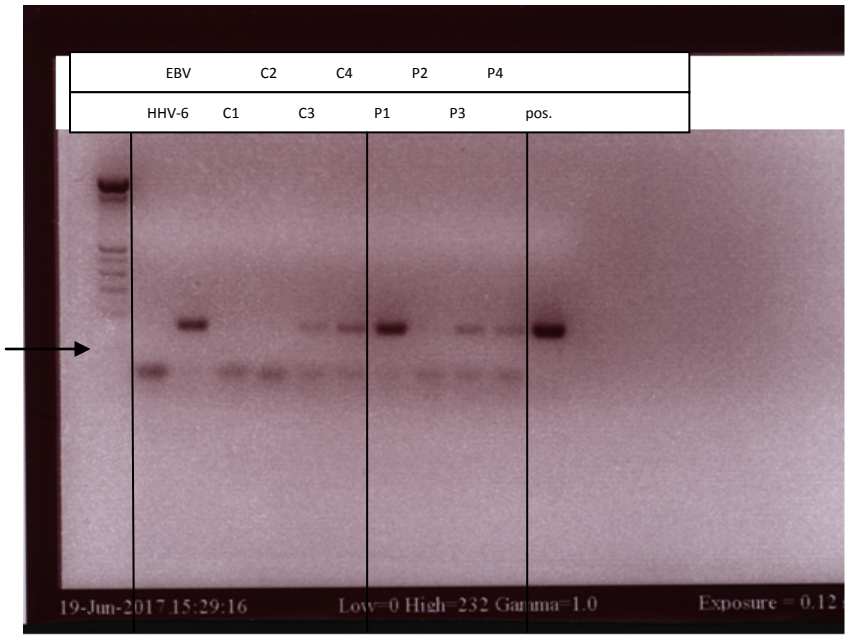

HHV-6: *Y278-00*
EBV: *Y281-00-1*
C1: *CMV 290-93-5*
C2: *CMV 234-93-9*
C3: *CMV 430-93-6*
C4: *CMV 118-94-1*
P1: *PML 214-98-8*
P2: *PML 471-93-6*
P3: *PML 342-93-5*
P4: *PML 97-93-8*
pos: *positive control RE Y304-12*

upper band: humanβ-actin (158 bp)
lower band: primers

(arrow indicating 100 bp)

***Fig. 18**: Analytic DNA gel electrophoresis for DNA quality analysis of unstained samples. Marker: 100 kb DNA ladder*

2.2 Detection of viral DNA in immunohistochemically treated sections

We also demonstrated that it is possible to isolate and identify specific DNA from paraffin-embedded virus encephalitis cases. We proceeded with a next step which was to examine possible determination of viral DNA in immunohistochemically treated sections stained for Hsp70. Cells in EBV (both of lymphoma and cell culture origin), PML and HSV-1 sections were Hsp70 stained. No CMV sections were taken as no positive PCR results were possible under unstained conditions. Only regions with accumulations of Hsp70 positive cells were scratched off the glass slides and were DNA extracted. DNA concentrations are quoted in Tab. 19. Compared to unstained samples (Tab. 18) those values are remarkably lower. In three cases (PML 97-93-8, HSV-1 67-83-2 and 204-83-1) DNA concentrations are slightly below the detection limit of the photospectrometer. In no case DNA concentrations is higher than 3.7 ng/µl. 260/280 sample purity seemed to be sound except in HSV-1 204-83-1. 260/230 ratios are out of the "pure" range as in the unstained sections (Tab. 18).

Virus copy number comparison of stained to unstained sections showed a diverse picture. In unstained PML section 97-93-8 1.7 x 10^4 copies were found while in the stained alternative it was 2.2 x 10^5. In unstained PML 214-98-8 it was 7.4 x 10^4 compared to 1.7 x 10^5 in the immunohistochemically treated section. In EBV case Y281-00-1 unstained 1.5 x 10^2 copies were detected while in the stained version it was 1.3 x 10^5. And in unstained HSV-1 section 67-83-2 a copy number of 2.4x10^4 was found compared to 1,1 x 10^3 in the unstained section of this case. In HSV-1 section 204-83-1 it was 1.3x10^7 copies unstained and 1,9 x 10^5 copies in the stained section.

As a matter of principle, danger of false-positive results has to be noticed when using viral primers. Due to their frequent homology to human DNA in consequence of a long co-evolution of both hosts and virus unintended products can be amplified. Tab. 20 has the results of the real-time PCR as copy numbers of viral-specific amplicons. The findings are contrasted to the determined copy numbers of unstained sections. Quantifications of both fractions was carried out at different time-points. The results reveal differences in the viral DNA quantification of unstained and stained paraffined sections of 1 to 2 magnitudes. Based on this observation, a DNA degrading influence of the immunohistochemical treatment could not be stated. Such effect could be at work in principal but is possibly overlain by methodic accuracy constraints of viral DNA identification by real-time PCR.

***Tab. 19**: Photospectrometric determination of DNA concentrations of Hsp70 stained samples*

EBV	**DNA conc.**	**A260 (RNA)**	**A280 (protein)**	**260/280 (sample purity)**	**260/230 (sample purity)**
281-00-1	2.3	0.045	0.025	1.84	1.05
EBV					
130-07-01	3.7	0.074	0.040	1.86	1.81
PML					
97-93-8	1.8	0.036	0.021	1.75	-3.06
214-98-8	2.6	0.053	0.028	1.92	1.26
HSV-1					
67-83-2	1.5	0.031	0.019	1.63	0.62
204-83-1	1.9	0.011	0.011	3.48	0.39
514-82-10	2.0	0.026	0.026	1.53	0.35

***Tab. 20**: Real-time PCR analysis of IHC untreated contrasted to treated (α-Hsp70 antibody) sections; indicated are numbers of copies (relating to 1/6 mass of entire section); in HSV-1 sample 514-82-10 no calculation was possible in 2nd test; ND = not done*

	IHC untreated	**IHC treated**
EBV		
130-07-01	ND	4.2×10^5
281-00-1	ND	1.3×10^5
CMV		
430-93-6	neg.	ND
118-94-1	neg.	ND
PML		
97-93-8	1.7×10^4	2.2×10^5
214-98-8	7.4×10^4	1.7×10^5
342-93-5	1.5×10^2	ND
EBV		
Y 281-00-1	1.4×10^7	1.3×10^5
HSV-1		
67-83-2	2.4×10^4	$1{,}1 \times 10^3$
204-83-1	1.3×10^7	$1{,}9 \times 10^5$
237-91-5	1.3×10^4	ND
330-82-4	4.7×10^5	ND
514-82-10	8.8×10^2	neg.
529-84-6	8.5×10^3	ND

To rule out false-positive results as much as possible, immunohistochemically treated samples were also probed by non-specific primers. Only those samples were taken that displayed feasible PCR results. PML sections 97-93-8, 214-98-8, EBV Y281-00-1, and HSV-1 67-83-2, 204-83-2 that were Hsp70 labeled and quantitatively real-time PCR amplified were subjected to additional real-time PCR testing by using non-specific primers. This procedure should exclude the possibility of false-positive binding of the primers. CMV-specific primers were used in all cases. CMV cases 234-93-9 and 290-93-5 had to be left out as material already was depleted. All samples were clearly negative for non-specific primers

Furthermore, recently received RE biopsy material was compared to such of longer storage to analyse the storage influence to DNA integrity. First, DNA was isolated from recently prepared sections from RE biopsy material (Y304-12, cut 12th of june, 2012). The sample covering a section area of about 2 cm^2 was cut 100 µm thick and was used entirely for extraction. Additionally, DNA of an older paraffined RE sample (N 565/08, biopsy date 2008-03-18, cutting date unknown, probably 2008) was isolated, the section having a regular

thickness of around 5 µm. According to manufacturer's (DAKO) instructions, Thickness and fixation duration are supposed to influence the DNA concentration crucially. Results of DNA concentration measurements can be found in Tab. 21. Values of both older and newer RE material were higher than in other encephalitic material tested (Tab. 18, Tab. 19). The older RE section of 5 µm thickness had a DNA concentration of 11.8 ng/µl while the newer section of 100 µm had 162 ng/µl. Sample purity can be considered acceptable. Products of the PCR using β-actin primers were subjected to gel electrophoretic analysis. The comparison showed a distinctively stronger band for the newer biopsy material (Fig. 19).

***Tab. 21**: Photospectrometric determination of DNA concentrations of RE comparison*

RE	DNA conc.	A260 (RNA)	A280 (protein)	260/280 (sample purity)	260/230 (sample purity)
N 565-08	11.8	0.236	0.103	2.29	1.83
304-12	102.4	2.047	1.071	1.91	2.30
304-12	162.0	3.240	1.692	1.92	2.26

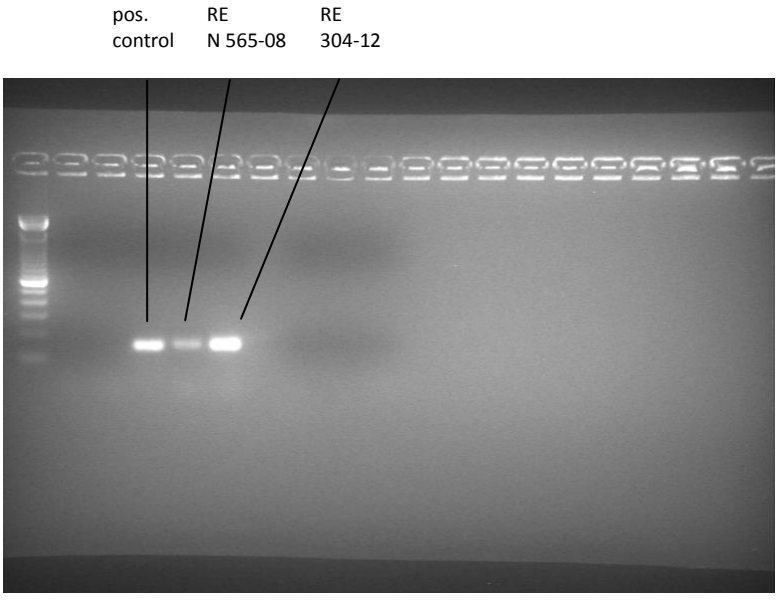

***Fig. 19**: Analytic DNA gel electrophoresis for comparison of DNA quality analysis of RE sections. β-actin specific primers were used. Positive control from live human umbilical vein endothelial cells (HUVECs). Marker: 100 kb DNA ladder.*

2.3 Detection of viral DNA in laser-capture microdissected stained cells

Finally, low numbers of Hsp70 or Hsp40 positive cells were isolated by laser-capture microdissection. Resulting low volumes of of total DNA was assessed to its constraints regarding positive identification of viral DNA in the various samples.

Pre-experiment

In a pre-experiment, Hsp70 marked cells in the distinct PML section 359-93-7A1 were microdissected and real-time PCR analyzed by using virus-specific primers. Paraffined sections with a thickness of around 5 µm were mounted to a nuclease and human nucleic acid free PET-membrane slide. The section was stained by α-Hsp70 antibody to show such cells with upregulated and nuclearly translocated Hsp70. Fig. 20 shows exemplary screen-shots from the microdissection procedure.

One fraction with 5 microdissected $Hsp70^+$ cells and one with 50 such cells were processed. Tab. 22 gives the photospectrometric determination of DNA parameters. The following descriptions include the constricting mathematical symbol "≈" as it is extremely difficult to calculate the exact number of microdissected cells due to the collecting procedure by the sticky isolation caps. In this pre-experiment, the difference in cell numbers did not find expression in the determined DNA concentrations of both fractions. Microdissection of ≈ 5 cells gave a DNA concentration of 5.3 ng/µl while ≈ 50 cells gave 4.1 ng/µl. 260/280 sample purity was acceptable, 260/230 ratio was again out of range as in the previous experiments (Tab. 18, Tab. 19). Possible reasons could be differing DNA quality and the number of virions as well as processing inhomogeneities/loss during DNA isolation. As no standards were available no quantification of PCR products was possible. Only qualitative real-time PCR analysis could be done. Positive control sections for EBV, HSV-1 and PML was material that was positively PCR tested by the AKH Department of Virology before. For the 5-cell fraction a C_q mean of 33.1 was measured. This value reached 33.44 for the 50-cell fraction (Tab. 23).

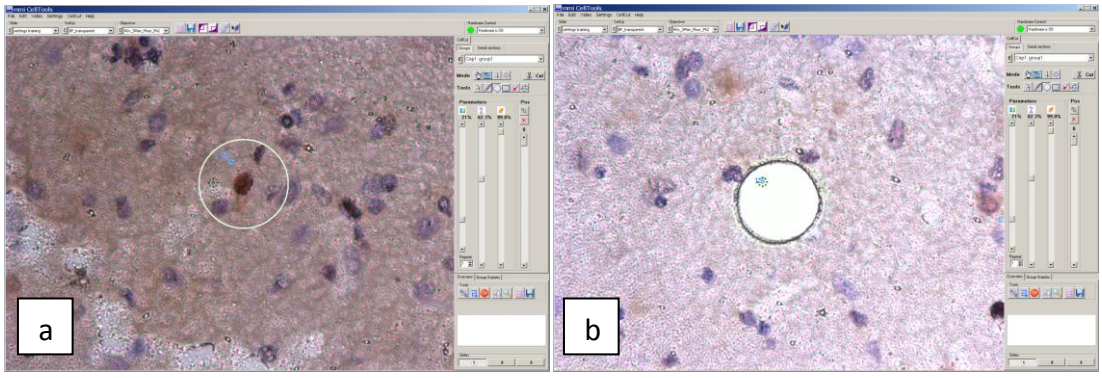

***Fig. 20**: Screen-shot from laser-capture application. Circle around $Hsp40^+$ cell (a) is microdissected (b).*

***Tab. 22**: Photospectrometric determination of DNA concentrations of laser-captured Hsp70$^+$ cells*

Hsp70$^+$ cells cut out	DNA conc.	A260 (RNA)	A280 (protein)	260/280 (sample purity)	260/230 (sample purity)
≈ 5	5.3	0.106	0.066	1.61	0.39
≈ 50	4.1	0.082	0.054	1.52	0.30

***Tab. 23**: Qualitative real-time PCR by TaqMan probes in PML case*

sample	C_q	C_q mean	C_q SD	number of Hsp70$^+$ cells cut out
359-93-7A1	32.90	33.10	0.278	≈ 5
"	33.29	33.10	0.278	duplicate
"	32.09	32.44	0.498	≈ 50
"	32.79	32.44	0.498	duplicate

Microdissection in CMV

Having becoming aware of its even better colocalization features as a surrogate marker for virally infected cells, Hsp40 stained sections were subjected to laser-capture after this pre-experiment. CMV and PML cases were taken due to their good previous staining results. CMV sections 290-93-5 and 430-93-7 could not be microdissected as no Hsp40$^+$ cells were found. This was consistent to former double-stainings, both light- and fluorescence-microscoped, where neither virus+ nor Hsp70$^+$ cells were found on these sections. Again, 5 and 50 labeled cells were cut out. Tab. 24 has the results of the microdissected Hsp40$^+$ cells in CMV cases.

In 62-94-9 and 455-92-7B no virus-specific amplicons were detected except for one sample of the fraction "≈ 50 Hsp40$^+$ cells". Case 559-92-11 was positive in all three fractions with one C_q value of the negative control even being very low = 11.96. In this section, presence of CMV DNA was found at around cycle 37. Unexpectedly, there did not seem to be much difference between isolation of 5 cells from isolation of 50 cells. As only this section was positive for Hsp40$^-$ microdissected cells the laser-capture was repeated. This was done together with that of PML sections described in Tab. 26. In this second run the sample was negative for existence of virus-specific amplicons in Hsp40$^-$ cells.

Furthermore, C_q mean of the fraction "≈ 50 Hsp40$^+$" compared to the C_q of the fraction "≈ 5 Hsp40$^+$" was lower by around 9 cycles which would reflect the increase in cell number (Tab. 25). A systemic negative control consisting of empty membrane from the slides appeared negative as was the PCR negative control of master-mix alone.

***Tab. 24**: Qualitative real-time PCR by TaqMan probes of Hsp40$^+$ cells in CMV cases*

sample	C_q	C_q mean	C_q SD	number of Hsp40$^+$ cells cut out
62-94-9	N/A	0.00	0.000	≈ 5
"	N/A	0.00	0.000	duplicate
"	37.22	37.22	0.000	≈ 50
"	N/A	0.00	0.000	duplicate
"	N/A	0.00	0.000	neg. con. (≈ 50 Hsp40$^-$ cells)
"	N/A	0.00	0.000	duplicate
455-92-7B	N/A	0.00	0.000	≈ 5
"	N/A	0.00	0.000	duplicate
"	N/A	0.00	0.000	≈ 50
"	N/A	0.00	0.000	duplicate
"	N/A	0.00	0.000	neg. con. (≈ 50 Hsp40$^-$ cells)
"	N/A	0.00	0.000	duplicate
559-92-11	37.13	36.83	0.425	≈ 5
"	36.53	36.83	0.425	duplicate
"	36.92	36.68	0.344	≈ 50
"	36.43	36.68	0.344	duplicate
"	11.96	24.58	17.856	neg. con. (≈ 50 Hsp40$^-$ cells)
"	37.21	24.58	17.856	duplicate
	N/A	0.00	0.000	systemic negative control *)
	N/A	0.00	0.000	duplicate
	N/A	0.00	0.000	PCR negative control
	N/A	0.00	0.000	duplicate

*) from 559-92-11, only preparation-free membrane dissected

***Tab. 25**: Repeated dissection of CMV 559-92-11*

559-92-11	N/A	0	0	≈ 5
"	41.42	41.42	0	duplicate
"	32.78	32.75	0.037	≈ 50
"	32.73	32.75	0.037	duplicate
"	N/A	0		neg. con. (≈ 50 Hsp40$^-$ cells)
"	N/A	0	0.	duplicate
	N/A	0	0	systemic negative control *)
	N/A	0	0	duplicate

Microdissection in PML

7 PML samples were immunohistochemically labeled by α-Hsp40 antibody and microdissected as in the CMV cases. Again ≈ 50 $Hsp40^-$ as well as ≈ 5 $Hsp40^+$ and ≈ 50 $Hsp40^+$ cells were cut out together with systemic negative controls (empty membrane of object slide). To rule out false-positive primer binding all PML samples including systemic negative control and master-mix negative control were subjected to additional real-time PCR negative controlling by using non-specific CMV primers. CMV case 559-92-11 (Tab. 25) was tested by using JC virus-specific primers. The results were clearly negative.

Findings of virus specific real-time PCR are shown in Tab. 26. PML cases 97-93-8, 358-93-6, 359-93-7A2 showed plausible signal increase proportional to the number of $Hsp40^+$ cells cut out. Unfortunately, apart from duplicate in 359-93-7A2 the samples with ≈ 50 non-labeled cells also showed significant reactivity. As all $Hsp40^-$ controls find themselves in a certain range this could point to some form of misreactivity. In cases 12-93-2 no ≈ 50 $Hsp40^+$ cells were microdissected as the membrane tore during procedure. C_q difference of ≈ 50$Hsp40^-$ cells and ≈ 5 $Hsp40^+$ cells was 5.8, hence showing some degree of proportionality, similar was case 47-93-3. Separate from the inexplicable signals in the immunohistochemically labeled samples this would deliver 5 out of 7 more or less feasible results. This explicability became even more apparent in the PML systemic negative control which also displayed a C_q = 40.53 (the duplicate was negative). To rule out autofluorescence effects of the PET membrane a control was run with only probes applied and without primers. No signal was detectable. The manufacturing company also advertises the membrane as having "negligible" autofluorescence. The observed proportionality in 5 out of 7 cases rather speaks against general contamination effects in DNA isolation or in PCR procedure. The systemic negative control C_q = 40.53 was clearly below all other positive samples, though. Despite the fact that the origin of its fluorescence signal could not be clarified this C_q value ≈ 40 was used as negative control reference. Under these circumstances the ≈ 50 $Hsp40^-$ cells in cases 358-93-6 and 359-93-7A2 could be classified as being negative, also in regard to their very low C_q standard deviation.

It remained unclear why two PML cases displayed values for ≈ 50 $Hsp40^-$ cells almost as high as this negative reference. In 103-93-8 a C_q of 38.21 was measured and in 278-93-6 a C_q of 34.69. Moreover, proportionality was not correct as both cases showed higher C_q values for ≈ 5 $Hsp40^+$ cells than for 50 $Hsp40^+$ cells. Possible explanations targeted different postmortem delays or varying fixation conditions. It also is unclear what exactly is the reason for a positive signal in these $Hsp40^-$ cells. A cause could be that although these cells did not express Hsp40 they still carried CMV DNA. This, however, is rather unlikely since those cells were captured in a region far away from that where CMV normally is located. CMV case 559-92-11 was applied PML-specific primers but did not deliver specific amplicons. This speaks against an unspecific amplification of a genomic homologue. Primer choice seemed to be sound. Tab. 27 shows the increase in C_q means from ≈ 50 $Hsp40^-$ cells to ≈ 5 $Hsp40^+$ cells as well as from ≈ 50$Hsp40^+$ cells to ≈ 5 $Hsp40^+$ cells. When the two samples without

proportionality are eliminated, the remaining exhibit adequate relations of magnitude. ≈ 50 Hsp40- fraction would show a C_q mean of 36.48, ≈ 5 Hsp40+ cells would have a C_q mean of 31.54, and ≈ 50 Hsp40+ cells a C_q of 29.12 (Tab. 28) . The decreasing C_q would fit to the increase in Hsp40 labeled nuclei. C_q of ≈ 50 $Hsp40^-$ cells is lower by 4.94 cycles, which would mean ≈ 31 copies more compared to the C_q of ≈ 5 $Hsp40^+$ cells. The difference from ≈ 5 $Hsp40^+$ to that of ≈ 50$Hsp40^+$ cells is 2.42 cycles meaning ≈ 5 more copies.

***Tab. 26**: Qualitative real-time PCR by TaqMan probes of $Hsp40^+$ cells in PML cases*

sample	C_q	C_q mean	C_q SD	number of $Hsp40^+$ cells cut out
12-93-2	28.93	28.66	0.388	≈ 5
"	28.39	28.66	0.388	duplicate
"	-	-	-	≈ 50
"	-	-	-	duplicate
"	34.55	34.43	0.166	neg. con. (≈ 50 $Hsp40^-$ cells)
"	34.31	34.43	0.166	duplicate
47-93-3	30.68	30.48	0.29	≈ 5
"	30.27	30.48	0.29	duplicate
"	31.71	32.48	1.082	≈ 50
"	33.24	32.48	1.082	duplicate
"	32.82	33.13	0.44	neg. con. (≈ 50 $Hsp40^-$ cells)
"	33.44	33.13	0.44	duplicate
97-93-8	37.95	38.31	0.516	≈ 5
"	38.68	38.31	0.516	duplicate
"	28.29	28.23	0.083	≈ 50
"	28.17	28.23	0.083	duplicate
"	35.55	35.44	0.156	neg. con. (≈ 50 $Hsp40^-$ cells)
"	35.33	35.44	0.156	duplicate
103-93-8	35.79	35.83	0.063	≈ 5
"	35.88	35.83	0.063	duplicate
"	37.69	38.21	0.733	≈ 50
"	38.73	38.21	0.733	duplicate
"	33.05	33.45	0.566	neg. con. (≈ 50 $Hsp40^-$ cells)
"	33.85	33.45	0.566	duplicate
278-93-6	34.41	34.38	0.043	≈ 5
"	34.35	34.38	0.043	duplicate
"	35.12	34.69	0.214	≈ 50
"	34.81	34.69	0.214	duplicate
"	32.86	32.67	0.265	neg. con. (≈ 50 $Hsp40^-$ cells)
"	32.48	32.67	0.265	duplicate

sample	C_q	C_q mean	C_q SD	number of Hsp40$^+$ cells cut out
358-93-6	28.67	28.69	0.027	≈ 5
"	28.71	28.69	0.027	duplicate
"	26.38	26.37	0.011	≈ 50
"	26.37	26.37	0.011	duplicate
"	37.65	38.04	0.549	neg. con. (≈ 50 Hsp40$^-$ cells)
"	38.43	38.04	0.549	duplicate
359-93-7A2	31.58	31.58	0.007	≈ 5
"	31.57	31.58	0.007	duplicate
"	28.8	29.4	0.343	≈ 50
"	29.28	29.4	0.343	duplicate
"	41.38	41.38	0	neg. con. (≈ 50 Hsp40$^-$ cells)
"	N/A	0	0	duplicate
	40.53	40.53	0	systemic negative control *)
	N/A	0	0	duplicate
	N/A	0.00	0.000	PCR negative control
	N/A	0.00	0.000	duplicate

***Tab. 27**: C_q mean differences in the different fractions*

	Δ C_q mean		
	50$^-$ to 5$^+$	5$^+$ to 50$^+$	assessment
12-93-2	5,8	no data	+
47-93-3	2,7	-2	+
97-93-8	-2,9	10,1	+
103-93-8	-2,4	-2,4	-
278-93-6	-1,7	-0,3	-
358-93-6	9,4	2,3	+
359-93-7A2	9,8	2,2	+

***Tab. 28**: C_q means with eliminated samples*

	50 Hsp40⁻ cells				5 Hsp40⁺ cells				50 Hsp40⁺ cells			
	C_q m.	C_q SD	C_q m.	C_q SD	C_q m.	C_q SD	C_q m.	C_q SD	C_q m.	C_q SD	C_q m.	C_q SD
12-93-2	34.43	0.166	34.43	0.166	28.66	0.388	28.66	0.388	no	data	no	data
47-93-3	33.13	0.44	33.13	0.44	30.48	0.29	30.48	0.29	32.48	1.082	32.48	1.082
97-93-8	35.44	0.156	35.44	0.156	38.31	0.516	38.31	0.516	28.23	0.083	28.23	0.083
~~103-93-8~~	~~33.45~~	~~0.566~~	~~33.45~~	~~0.566~~	~~35.83~~	~~0.063~~	~~35.83~~	~~0.063~~	~~38.21~~	~~0.733~~	~~38.21~~	~~0.733~~
~~278-93-6~~	~~32.67~~	~~0.265~~	~~32.67~~	~~0.265~~	~~34.38~~	~~0.043~~	~~34.38~~	~~0.043~~	~~34.69~~	~~0.214~~	~~34.69~~	~~0.214~~
358-93-6	38.04	0.549	38.04	0.549	28.69	0.027	28.69	0.027	26.37	0.011	26.37	0.011
359-93-7A2	41.38	41.38	0	0	31.58	0.007	31.58	0.007	29.4	0.343	29.4	0.343
means	36.48				31.54				29.12			

Δ = 4.94 cycles ≈ 30.7 copies

Δ = 2.42 cycles ≈ 5.4 copies

Interpretation

Goal of this work was to investigate whether Hsp70 and Hsp40 chaperones can be used as surrogate markers for immunohistochemical identification of cells infected by DNA viruses. These heat-shock proteins, ubiquitous in eukaryotic cells, bacteria and many archaea, play a crucial role in times of cellular stress. Hsp70 and its co-chaperone Hsp40 are responsible for the correct folding and activation of many premature proteins as well as for the assembly of multi-protein complexes. Hsp40 delivers the nascent polypeptide chain to ATP-bound, inactive Hsp70 and hydrolyzes it. This conformational change to ADP-bound Hsp70 increases its substrate specificity for unfolded proteins and prevents them from aggregating. ADP is released by a Hsp70-specific nucleotide exchange factor. Virus replication process depends on Hsp70 and Hsp40 in aspects as protein synthesis and virion assembly[13].

Upregulation and nuclear translocation of these chaperones as stress responses to viral infections were observed *in vitro* in many cases before, i. e. by Jindal et al.[26] In 2004, Burch and Weller described the redistribution of Hsp70, its constitutively expressed form Hsc70, and Hsp40 to foci within the nuclei of Herpes simplex virus type 1-infected cells[8]. Prior to that, induction and translocation of Hsp70 in CMV-infected cells were observed by Ohgitani[27]. Devireddy et al showed a similar effect in JC virus infected cells when they reported that the Bcl-2 interacting protein BAG-1 activates expression of this virus. The BAG-1 family is known to be able to modulate chaperone activity of Hsc70 and Hsp70[27]. Mayer[13] also states various references for the induction of *hsp70* transcription by the Herpesviridae HSV-1, Varizella Zoster virus, CMV, and EBV. Furthermore, Brown et al revealed that Hsp70 is recruited to lipid-raft membranes of during respiratory syncytial virus replication[12].

Associations between Hsc70 and Papillomavirus assembly were also shown by Florin[11]. Immunohistochemical and PCR-based evaluation was carried out to prove these previous results concerning heat-shock proteins in vivo.

1. Immunohistochemical testing of Hsp70 and Hsp40 by virus-specific markers

Chaperones Hsp70 and Hsp40 were assessed in their ability to act as markers for DNA virus infected cells. The findings point to a clear coincidence of upregulation and nuclear translocation of Hsp70 and Hsp40 in DNA virus infected cells *in situ* as was seen in *in vitro* studies before.

Immunohistochemical analysis of Hsp70 and Hsp40 reactivity of autopsy material of CMV encephalitis and JC virus encephalitis patients showed that infected cells are clearly stronger stained in nucleus and cytoplasm than uninfected cells and that uninfected cells do not show clear translocation of Hsp70 and Hsp40 to their nuclei.

Quantification of colocalized Hsp70 and virus specific markers revealed average ratios of 45.8 % in the examined CMV sections and 45.5 % and 47.9 %, respectively, depending on the applied antibody, in the PML sections.

An average of only 16.1 % of HSV-1 infected cells showed nuclear translocalisation of Hsp70 and could therefore be identified as virus-infected by using Hsp70 staining. This deviance might be due to post-mortem delays of the autopsy material or to effects caused by the fixation conditions. In EBV-specifically marked cells, translocation of upregulated Hsp70 or Hsp40 chaperones to the nucleus was observed in only 3.8 % and 1.6 %, respectively, depending on the antibody. These values could reflect technical problems as background staining was intense. By now, we would not exclude that Hsp70 and Hsp40 could function as markers for EBV infected cells. In Measles virus infections no colocalizations were visible where according to Mayer[13] Hsp70 should play an important role in envelope protein folding and maturation.

Nuclearly conspicuous Hsp40 was detected in CMV and PML material in even larger extent. In an mean average of 56.2 % of CMV cases such co-occurrence was shown while in PML this even reached to 94.6 %. More than 1 out of 2 CMV cells had co-chaperone Hsp40 upregulated and translocated to their nucleus while in PML nearly every virus-infected cell did so. These findings strongly support the principal ability of Hsp70 and Hsp40 to mark DNA virus-infected cells.

2. Virus-specific PCR detection of isolated Hsp70 and Hsp40 positive cells

Aim of the laser-capture microdissection of $Hsp40^{+}$ nuclei in CMV and PML sections was to confirm that selection of cells based on Hsp40 stainings indeed can be used to locate and

identify virus-infected cells. Method of choice was the TaqMan real-time PCR by virus-specific primers. The Taq polymerase is frequently used for such detections as its synthesis rate is relatively high compared to the Pfu polymerase. Disadvantage of the Taq polymerase is its missing proof-reading activity.

Real-time PCR results were difficult to classify. We microdissected ≈ 5 $Hsp40^+$ cells as well as ≈ 50 of these. In CMV three samples were examined. In one case we could not demonstrate the presence of CMV sequences at all while the second case delivered only weakly detectable viral DNA when 50 cells were microdissected. When a third case with a positive negative control was re-tested it showed adequate results. The fraction of 50 positive cells appeared with a higher amount of viral DNA that the fraction of 5 cells. Similar problems in CMV samples already occurred in pre-experiments where entire material was taken. When this material was subjected to virus copy quantification by real-time PCR no positive results were obtained at all. The use of different CMV primers should be reconsidered.

In PML, unexpectedly, systemic negative control was positive, a phenomenon that could not be clarified. We accepted the C_q = 40.53 (45 cycles) of this control to be set as negative control. 5 out of 7 samples showed useful results when doing so. The acceptance of this positive negative control already was explained in "Results". Its C_q = 40.53 was clearly above the C_q values of all other positive samples. We decided to treat this value as being false-positive. 5 out of 7 cases showed proportionality of viral DNA amounts regarding to the number of microdissected cells. This plausibility made contanimations effects improbably. As mentioned, the cause of the fluorescence signal in the systemic negative controls remained unclear. López-Ríos et al. reported on a high risk of false-positive DNA PCR results in SV40 infections as primers can bind to common laboratory plasmids when not carefully designed[28]. This danger could be ruled out as only a qualitative real-time PCR was conducted without use of plasmids. Further literature research has not revealed hints to the cause of this phenomenon or the use of false-positive controls.

In general, there may be diverse reasons for the difficult real-time PCR detection of viral DNA in $Hsp70^+$ or $Hsp40^+$ cells. The influence of post-mortem delays and fixation conditions might also affect DNA integrity as can the immunohistochemical staining procedure, i. e. steaming bath treatment for retrieval of antigens and appliance of H_2O_2 as quencher of endogenous peroxidase.

3. Conclusion and future prospects

The identification of DNA virus-infected cells by using Hsp70 or Hsp40 chaperones as surrogate markers seems to be functional. Qualitative immunohistochemical analysis shows CMV and JC virus infected cells stronger stained in their nucleus and cytoplasm compared to uninfected cells. In addition, uninfected cells lack to exhibit translocation of Hsp70 and Hsp40 to their nucleus. In roughly every second Hsp70 or Hsp40 positive nucleus a CMV

marker reactivity was observed. This colocalization was even stronger in PML where Hsp40 is upregulated and translocated to the nuclei in nearly every case. Unfortunately, this was not confirmable in HSV-1 despite principal *in vitro* validation. It would be interesting to analyze differently fixated tissue samples from these encephalitic infections. In EBV different pre-treatment conditions should be tried out. Regarding a possible real-time PCR confirmation of these results we see that further research has to be done. Current PCR findings do not clearly demonstrate that virally infected cells could be isolated. First, the problem of the false-positive PML results has to be solved. Therefore, it would be necessary to optimize DNA isolation processing after microdissection. The number of analyzed samples could be increased. In CMV different primer sets could be tried. It also would be worth a try whether another laboratory confirms the TaqMan real-time PCR results. A fascinating outlook regards to the application of Hsp70 and Hsp40 as surrogate markers in DNA viruses unidentified so far. This could maybe enable falsification of controversial hypotheses as i. e. the aetiology of Rasmussen encephalitis where laser-capture microdissection and subsequent sequencing could reveal a viral cause of the disease.

Hsp70 and Hsp40 can certainly discriminate uninfected from infected cells, depending on the virus while in HSV-1 for some kind of reason this does not work. Technical problems in PCR analysis seem to prevent a genetic confirmation.

Acknowledgments

I would like to say "thank you" to my supervisor Prof. Jan Bauer, whose affable assistance helped to make this work possible. Also always a lending hand for me had Marianne Leißer, Ulrike Koeck, MSc., and Angela Kury from the Histology Lab as well as Phd students Simon Hametner, Cornelia Schuh, Isabella Wimmer and Maja Kitic. Eventually, supportive were department head Prof. Dr. Hans Lassmann, Prof. Dr. Monika Bradl, Mag. Regina Hirnschall, and Gertrude Makkos. I also would like to thank Prof. Dr. Stephan Aberle, Prof. Dr. Reginald Bittner, Ass. Prof. Dr. Wolfgang Schmidt, Sandra Dysek, and last but not least Manuela Haberl for their great help.

Literature

[1] Oguni et al, "The natural history of the syndrome of chronic encephalitis and epilepsy: a study of the MNI series of fortyeight cases", in Andermann "Chronic encephalitis and epilepsy. Rasmussen syndrome", Boston: Butterworth-Heinemann (1991) 7 – 35

[2] Granata et al, "Rasmussen encephalitis", Neurol 60 (2003), 422 – 425

[3] Bien et al, "The natural history of Rasmussen encephalitis", Brain 125 (2002), 1751 – 1759

[4] Bien et al, "Destruction of Neurons by Cytotoxic T Cells: A New Pathogenic Mechanism in Rasmussen Encephalitis", Ann Neurol 51 (2002), 1 – 8

[5] Bauer et al, "Astrocytes Are a Specific Immunological Target in Rasmussen Encephalitis", Ann Neurol 61 (2007), 1 – 15

[6] Burch et al, "Nuclear Sequestration of Cellular Chaperone and Proteasomal Machinery during Herpes Simplex Virus Type 1 Infection", J Virol 78 (13) (2004), 7175 – 7185

[7] Livingston et al, "Virus-Induced Chaperone-Enriched (VICE) Domains Function as Nuclear Protein Quality Control Centers during HSV-1 Infection, PLOS Pathogens (2009-10-09)

[8] Burch et al, "Herpes Simplex Virus Type 1 DNA Polymerase Requires the Mammalian Chaperone Hsp90 for Proper Localization to the Nucleus", J Virol 79(16) (2005), 10740 – 10749

[9] Koskinen et al, "Nuclear Colocalization of Cellular and Viral *myc* Proteins with Hsp70 in *myc*-Overexpressing Cells, J Virol, Vol. 65 (1991), 842 – 851

[10] Florin et al, "Nuclear Colocalization of Papillomavirus Minor Capsid Protein L2 Requires Hsp70", J Virol 78 (11) (2004), 5546 – 5553

[11] Brown et al, "Evidence for an association between heat shock protein 70 and the respiratory syncytial virus polymerase complex within lipid-raft membranes during virus infection", Virol 338 (2005), 69 – 80

[12] Mayer et al, "Hsp70 chaperones: Cellular functions and molecular mechanism", Cell Mol Life Sci 62 (2005), 670 – 684

[13] Mayer, "Recruitment of Hsp70 chaperones: a crucial part of viral survival strategies", Rev Physiol Biochem Pharmacol 153 (2005), 1 – 46

[14] Knox et al, "Heat shock protein 40 (Hsp40) plays a key role in the virus life cycle", Virus Res 160 (2011), 15 – 24

[15] Strick et al, "Management of herpes simplex virus type 2 infection in HIV type 1-infected persons", Clin Infect Dis 43 (3) (2006), 347 – 356

[16] Chayavichitsilp et al, " Herpes simplex", Pediatr Rev 30 (4) (2009), 119 – 129

[17] Whitley et al, "Herpes Simplex Virus", in Scheld et al "Infections of the Central Nervous System" (1997), Philadelphia: Lippincott-Raven, 73 – 89

[18] Bierman et al, "Non-Hodgkin's lymphoma", in Goldman et al "Cecil Medicine" (2011), Philadelphia: Saunders Elsevier, 191

[19] Muñoz-Mármol et al, " JC virus early protein detection by immunohistochemistry in progressive multifocal leukencephalopathy: a comparative study with in situ hybridization and polymerase chain reaction", J Neuropathol Exp Neurol 63 (11) (2004), 1124 - 1130

[20] King et al, "A highly sensitive detection method for immunohistochemistry using biotinylated tyramine", J Pathol 183 (1997), 237 – 241

[21] Schmitt et al, "Comparison of contrast, sensitivity and efficiency of signal amplified and nonamplified immunohistochemical reactions suitable for videomicroscopy-based quantification and neuroimaging", Brain Res Protocols 12 (2004), 157 – 171

[22] Oghitani et al, "Biphasic translocation of a 70 kDa heat shock protein in human cytomegalovirus-infected cells", J Gen Virol 80 (1999), 63 – 68

[23] Burch et al, "Herpes Simplex Virus Type 1 DNA Polymerase Requires the Mammalian Chaperone Hsp90 for Proper Localization to the Nucleus", J Virol 79 (16) (2005), 10740 – 10749

[24] Morgello et al, "Cytomegalovirus encephalitis in patients with acquired immunodeficiency syndrome: An autopsy study of 30 cases and a review of the literature", Human Path 18 (3) (1987, 289 – 297

[25] Murayama et al, " Neuropathology of progressive multifocal leukoencephalopathy", Brain Nerve 59 (2), (2007), 119 - 124

[26] Jindal et al, "Stress responses to viral infection", Trends Microbiol 2 (1994), 89 – 91

[27] Devireddy et al, "BAG-1, a novel Bcl-2 interacting protein, activates expression of human JC virus", J Gen Virol 81 (2) (2000), 351 – 357

[28] López-Ríos et al, "Evidence against a role for SV40 infection in human mesotheliomas and high risk of false-positive PCR results owing to presence of SV40 sequences in common laboratory plasmids", The Lancet 364 (9440) (2004), 1157 – 1166